MANUSCRIPT TITLE

Affinity-tagged SMAD1 and SMAD5 mouse lines reveal transcriptional reprogramming mechanisms during early pregnancy

AUTHORS

Zian Liao[a,b,c,d], Suni Tang[a,d], Kaori Nozawa[a,d], Keisuke Shimada[e], Masahito Ikawa[e], Diana Monsivais*[a,d], and Martin M. Matzuk*[a,b,c,d]

[a]Department of Pathology & Immunology, Baylor College of Medicine, Houston, TX, 77030, USA
[b]Department of Molecular and Human Genetics, Baylor College of Medicine, Houston, TX, 77030, USA
[c]Graduate Program of Genetics and Genomics, Baylor College of Medicine, Houston, TX, 77030, USA
[d]Center for Drug Discovery, Baylor College of Medicine, Houston, TX, 77030, USA
[e]Research Institute for Microbial Diseases, Osaka University, Osaka, 565-0871, Japan

*To whom correspondence should be addressed to: Martin M. Matzuk, MD, PhD Tel: +1 713-798-6451; Fax: +1 713-798-5838; Email: mmatzuk@bcm.edu; and Diana Monsivais, PhD Tel: +1 713-798-1279; Fax: +1 713-798-5838; Email: diana.monsivais@bcm.edu.

KEY WORDS: uterus, decidualization, SMAD proteins, bone morphogenetic proteins, progesterone, endometrium

ABSTRACT

Endometrial decidualization, a prerequisite for successful pregnancies, relies on transcriptional reprogramming driven by progesterone receptor (PR) and bone morphogenetic protein (BMP)-SMAD1/SMAD5 signaling pathways. Despite their critical roles in early pregnancy, how these pathways intersect in reprogramming the endometrium into a receptive state remains unclear. To define how SMAD1 and/or SMAD5 integrate BMP signaling in the uterus during early pregnancy, we generated two novel transgenic mouse lines with affinity tags inserted into the endogenous SMAD1 and SMAD5 loci (*Smad1*$^{HA/HA}$ and *Smad5*$^{PA/PA}$). By profiling the genome-wide distribution of SMAD1, SMAD5, and PR in the mouse uterus, we demonstrated the unique and shared roles of SMAD1 and SMAD5 during the window of implantation. We also showed the presence of a conserved SMAD1, SMAD5, and PR genomic binding signature in the uterus during early pregnancy. To functionally characterize the translational aspects of our findings, we demonstrated that SMAD1/5 knockdown in human endometrial stromal cells suppressed expressions of canonical decidual markers (*IGFBP1, PRL, FOXO1)* and PR-responsive genes (*RORB*, *KLF15)*. Here, our studies provide novel tools to study BMP signaling pathways and highlight the fundamental roles of SMAD1/5 in mediating both BMP signaling pathways and the transcriptional response to progesterone (P4) during early pregnancy.

63 **INTRODUCTION**

64 Infertility is an emerging health issue that affects approximately 15% of couples[1]. One in five women
65 aged 15 to 49 years old with no prior births suffers from infertility in the United States[2]. One important
66 factor affecting fertility is failed embryo implantation or subsequent post-implantation loss due to
67 endometrial defects. This is evident from the high number of failed pregnancies, with as many as 15% of
68 pregnancies resulting in early pregnancy losses[3]. Understanding the molecular mechanism of how the
69 maternal endometrium becomes suitable for embryo implantation and eventual decidualization, will be
70 the key to eradicating global concerns related to infertility and early pregnancy losses.

71 The transforming growth factor β (TGFβ) family plays diverse roles in development, physiology, and
72 pathophysiology[4,5], and in particular, signaling pathways downstream of the bone morphogenetic protein
73 (BMP) subfamily are essential for decidual formation[6,7]. There are more than 30 TGFβ family ligands,
74 and these ligands signal through complexes of transmembrane type 1 Activin-Like Kinases (ALK)
75 receptors (ALK1, ALK2, ALK3, ALK6) and transmembrane type 2 receptors (BMPR2, ACVR2A,
76 ACVR2B) and then phosphorylate downstream SMAD1 and SMAD5 proteins. Phosphorylated SMAD1/5
77 form heteromeric complexes with SMAD4 and translocate to the nucleus to induce specific transcriptional
78 programs. Our laboratory and others have used genetically engineered mouse models with deletions of
79 ligands, receptors, and downstream effectors of BMP signaling pathways to establish that BMP signaling
80 pathways are major regulators of early pregnancy[6-12].

81 A successful pregnancy begins with reciprocal crosstalk between the maternal endometrium and the new
82 blastocyst during the peri-implantation window. Effective implantation requires precise synchronization
83 between the development of the blastocyst and the transformation of the maternal endometrium into a
84 functional decidua. Endometrial stromal fibroblasts undergo the decidualization process in which they
85 differentiate into unique secretory decidual cells that offer a supportive and immune-privileged
86 microenvironment required for embryo implantation and placental development. Decidualizing stromal
87 cells can react to individual embryos in a way that either supports the implantation and subsequent
88 embryonic development or exerts early rejection[13,14]. Aberrant decidualization processes are observed in
89 patients with recurrent pregnancy loss (RPL), displaying a disordered pro-inflammatory response,
90 decreased induction of decidual marker genes, and abnormal responses to embryonic human chorionic
91 gonadotropin[13,15,16]. In addition to affecting early pregnancy outcomes, defective decidualization is also
92 involved in the maternal etiology of preeclampsia, causing abnormal placental phenotype[17,18]. The
93 process of decidualization is tightly regulated by hormone signaling pathways (estrogen, E2, and
94 progesterone, P4), as well as by BMP signaling pathways. Our recent studies found that endometrial
95 *Smad1* deletion had no significant effect on fertility, *Smad5* conditional deletion resulted in subfertility,
96 while double *Smad1/5* conditional deletion led to infertility due to implantation and decidualization
97 defects[9]. The uteri of mice with double conditional *Smad1/5* deletion also displayed decreased response

98 to P4 during the window of implantation, suggesting synergy between the two pathways. However, the
99 mechanistic genomic actions of SMAD1 and/or SMAD5 in the uterus have not been explored, partly
100 because there are no specific antibodies that distinguish phospho-SMAD1 versus phospho-SMAD5.

101 In this study, we define how SMAD1/5 instructs the decidualization process using genomic approaches in
102 newly generated transgenic mouse lines. We inspect the potential crosstalk between P4 and BMP
103 signaling pathways mediated by SMAD1/5. Together, our study demonstrates that SMAD1 and SMAD5
104 exhibit shared and unique genomic binding features and further reveals that SMAD1/5 contributes to the
105 P4 response through transcriptional reprogramming during decidualization.

106 MATERIALS AND METHODS

107 Generation of Knock-in Mouse Lines

108 *Smad5*$^{PA/PA}$ knock-in (KI) mice were generated using a similar approach as previously described[19].
109 Briefly, single-guide RNA (sg-RNA) was designed to target the regions close to the start codon (Figure
110 1A,B) and the sgRNA sequence was inserted into the pX459 V2.0 plasmid (#62988, Addgene). The
111 reference plasmids containing PA tag sequence were constructed in pBluescript II SK (+) vector (Agilent,
112 Palo Alto, CA, USA). One µg of guide RNA inserted vector and 1.0 µg of reference plasmid were co-
113 transfected into EGRG01 embryonic stem (ES) cells. Twelve ES clones out of 48 had the expected
114 knock-in allele. ES cell clones that possessed the proper KI allele were injected into ICR embryos and
115 chimeric blastocysts were transferred into pseudopregnant females. Chimeric male mice were mated
116 with B6D2F1 female mice to obtain the PA-tagged SMAD5 KI heterozygous mice. Homozygous
117 *Smad5*$^{PA/PA}$ mice were maintained in the C57BL/6 J × 129S5/SvEvBrd mixed genetic background. To
118 generate *Smad1*$^{HA/HA}$ mice, Cas9 protein (Thermo Fisher, A36497), sg-RNA, and a repair oligo of
119 homology-directed repair (HDR) containing HA-tag and linker sequences were electroporated into
120 zygotes harvested from *in vitro* fertilization using B6D2F1 male and female mice. An ECM830
121 electroporation system (BTX, Holliston, MA) was used for electroporation. Subsequently, embryos were
122 cultured overnight to the 2-cell stage and then transferred to the oviducts of pseudopregnant CD-1 mice
123 (Center for Comparative Medicine, Baylor College of Medicine). Pups were further screened for
124 successful heterozygous or homozygous knock-in alleles by PCR using primers spanning across the HA
125 tag. Sequences of sgRNA, the single-stranded repair oligo for HDR and primer used for genotype are
126 listed in Supplementary Table 1.

127 Animal ethics compliance and tissue collection

128 All mice were housed under standard conditions of a 12-hour light/dark cycle in a vivarium with controlled
129 ambient temperature (70˚F ± 2˚F and 20-70% relative humidity). All mouse handling and experimental
130 procedures were performed under protocols approved by the Institutional Animal Care and Use

131 Committee of Baylor College of Medicine. All experiments were performed with female mice aged
132 between 7 to 12 weeks with a C57BL/6 J × 129S5/SvEvBrd mixed genetic background. All mice were
133 euthanized using isoflurane induction followed by cervical dislocation, and tissues were snap-frozen in
134 liquid nitrogen.

135 **Cleavage Under Targets and Release Using Nuclease (CUT&RUN) Approach**

136 Nuclei from uterine tissues were purified following a previously published protocol[20]. The experiments
137 were performed using pooled biological replicates from two mice that were processed as technical
138 replicates throughout the CUT&RUN procedure and analysis. In short, uteri were harvested from
139 pregnant mice at 4.5 days post coitus and washed with cold swelling buffer (10 mM Tris-HCl pH 7.5,
140 2 mM $MgCl_2$, 3 mM $CaCl_2$, 1X Protease Inhibitor Cocktail (PIC, Roche, 11836170001)) immediately after
141 collection. Then tissue was cut into small pieces (~2-3mm) using scissors, while submerged in cold
142 swelling buffer. Nuclear extract was prepared by dounce homogenization in cold swelling buffer (using a
143 size 7 dounce) and filtered using the cell strainer (100 µm, BD Biosciences). Lysate was centrifuged at
144 400 g for 10 min, then resuspended in lysis buffer (swelling buffer with 10% glycerol and 1% CA-630, 1X
145 PIC) using end-cut or wide-bore tips and incubated on ice for 5 min. Nuclei were washed twice with lysis
146 buffer and resuspended in lysis buffer. Next, CUT&RUN procedure largely follows a previous protocol[21].
147 Briefly, around 500,000 nuclei were used per reaction. 10 µl of concanavalin-coated beads (Bangs Labs,
148 BP531) were washed twice in Bead Activation Buffer (20 mM HEPES, pH 7.9, 10 mM KCl, 1 mM $CaCl_2$,
149 1 mM $MnCl_2$) for each reaction. Then, beads were added to nuclei resuspension and incubated for 10
150 mins at room temperature. After incubation, bead-nuclei complexes were resuspended in 100 µl
151 Antibody Buffer (20 mM HEPES, pH 7.5, 150 mM NaCl, 0.5 mM Spermidine, 1X PIC, 0.01% digitonin,
152 and 2mM EDTA) per reaction. One µg of IgG antibody (Sigma, I5006), HA antibody (EpiCypher, 13-
153 2010), PA antibody (Fuji Film, NZ-1) and PR antibody (Cell Signaling, D8Q2J) were added to each group
154 respectively. After overnight incubation at 4 °C, bead-nuclei complexes were washed twice with 200 µl
155 cold Dig-Wash buffer (20 mM HEPES pH=7.5, 150 mM NaCl, 0.5 mM Spermidine, 1X PIC, 0.01%
156 digitonin) and resuspended in 50 µl cold Dig-Wash buffer with 1 µl pAG-MNase (EpiCypher, 15-1016)
157 per reaction. After incubation at room temperature for 10 min, bead-nuclei complexes were washed twice
158 with 200 µl cold Dig-Wash buffer and resuspended in 50 µl cold Dig-Wash buffer, then 1 µl 100 mM
159 $CaCl_2$ was added to each reaction. The mixture was incubated at 4 °C for 2 hours and the reaction was
160 stopped by adding 50 µl Stop Buffer (340mM NaCl, 20 mM EDTA, 4 mM EGTA, 0.05% Digitonin, 100
161 ug/mL RNase A, 50 mg/mL glycogen, 0.5 ng E. coli DNA Spike-in (EpiCypher, 18-1401)) and incubate at
162 37 °C for 10 min. The supernatant was collected and subjected to DNA purification with phenol-
163 chloroform and ethanol precipitation. Sequencing libraries were prepared using NEBNext Ultra II DNA
164 Library Prep Kit (New England BioLabs, E7645) following manufacture's protocol. Paired-end 150 bp
165 sequencing was performed on a NEXTSeq550 (Illumina) platform.

166 **Bioinformatic Analysis for CUT&RUN data and re-analysis of published single-cell RNA seq data**

167 For CUT&Run data, raw data were de-multiplexed by bcl2fastq v2.20 with fastqc for quality control.
168 Clean reads were mapped to reference genome mm10 by Bowtie2, with parameters of --end-to-end --
169 very-sensitive --no-mixed --no-discordant --phred33 -I 10 -X 700. For Spike-in mapping, reads were
170 mapped to E. coli genome U00096.3. Duplicated reads were removed, and only uniquely mapped reads
171 were kept. Spike-in normalization was achieved through multiply primary genome coverage by scale
172 factor (100000 / fragments mapped to E. coli genome). CUT&RUN peaks were called by SECAR[22] with
173 the parameters of -norm -stringent -output. Track visualization was done by bedGraphToBigWig[23], bigwig
174 files were imported to Integrative Genomics Viewer for visualization. For peak annotation, common
175 peaks were identified with 'mergePeaks' function in HOMER v4.11[24] and then genomic annotation was
176 added by ChIPseeker [25]. Motif analysis was conducted through HOMER v4.11 with parameter set as
177 findMotifsGenome.pl mm10 -size 200 -mask[24]. Peak heatmaps were plotted using deepTools 2.4.2 with
178 clustering options set to k-means[26]. For single-cell RNA seq, raw data was obtained from EMBL-EBI
179 under accession No. E-MTAB-10287. Cells with low coverage (less than 500 genes detected) were
180 filtered, then gene counts were normalized for each cell by converting counts to quantiles and obtaining
181 the corresponding values from a normal distribution. Then normalized cell vectors are concatenated
182 along the gene panel. Plot visualization was conducted through CELLXGENE platform.[27]

183 **Western Blot Analysis of Immunoprecipitation (IP-WB)**

184 Tissues were pulverized in liquid nitrogen and then lysed using NETN buffer (20 mM Tris-HCl, pH 8.0,
185 150 mM NaCl, 0.5 mM EDTA, 10% Glycerol, and 0.5% NP-40). Protein concentration was determined by
186 BCA Protein Assay Kit (Thermo Fisher, 23225). 1.5 mg of total protein lysate was used for IP. IP was
187 performed by adding HA antibody (Cell Signaling, C29F4) or PA antibody (Fuji Film, NZ-1) to the lysate
188 and incubate for 1 hour at 4 °C. Subsequently, protein G magnetic beads (Thermo Fisher, 88847) were
189 added for an additional 1 hour at 4 °C. Then, the beads were washed five times with NETN buffer, and
190 denatured in sample buffer (Thermo Fisher, NP0007) for further analysis by Western blot. For western
191 blot procedures, briefly, denatured protein lysates were run on the 4 to 12%, Bis-Tris protein gels
192 (Thermo Fisher, NP0321BOX) followed by electrophoretic transfer to nitrocellulose membrane. The
193 membrane then went through blocking by 5% milk in Tris-buffered saline with Tween20 (TBST), followed
194 by incubation overnight at 4 °C in the primary antibodies anti-HA (Cell Signaling, C29F4), anti-PA (Fuji
195 Film, NZ-1), anti-SMAD1 (Life technologies, 385400) and anti-SMAD5 (ProteinTech, 12167-1-AP) at
196 1:1,000 dilution. The next day, membranes were washed three times with TBST, then incubated with
197 horseradish peroxidase–conjugated secondary antibody for 1 h at room temperature, then washed three
198 times with TBST, developed and imaged on iBright Imaging System (FL1500).

199 **Primary endometrial stromal cells isolation/RNAi/decidualization**

200 Studies using human specimens were conducted as indicated in a protocol approved by the Institutional
201 Review Board at Baylor College of Medicine, H-51900. Human endometrial stromal cells were collected
202 from healthy volunteers' menstrual effluent as previously reported[28-30]. (N=3) In brief, samples were
203 collected by participants in a DIVA cup during the 4-8 hours on the first night of menses and stored in
204 DMEM/F12 with 10% FBS, antibiotic/antimycotic and 100μg/ml Primocin in a cold insulated pack until
205 processing in the laboratory on the day of collection. The effluent was digested with 5 mg/ml collagenase
206 and 0.2 mg/ml DNase I for 20 min at 37 °C, then the cell pellet was collected by centrifuging at 2,500 rpm
207 for 5 min at room temperature. Next, red blood cell lysis was performed by resuspending the cell pellet in
208 20 ml of 0.2% NaCl for 20 seconds and neutralized with 20 ml of 1.6% NaCl. Then the solution was then
209 centrifuged at 2,500 rpm for 5 min. Five ml complete medium (DMEM/F12 supplement with 10% FBS, 1X
210 Antibiotic-Antimycotic + 100 μg/ml Primocin) was used to resuspend the pellet and the solution was
211 passed through 100 μm and 20 μm cell strainer sequentially. The flowthrough containing the stromal
212 cells was centrifuged for 5 min at 2,500 rpm and the pellet was resuspended in 10 ml complete medium
213 and plated in a 10 cm dish. siRNA knockdown was performed using Lipofectamine RNAiMAX following
214 the manufacturer's protocol. In brief, 0.2 million stromal cells were plated in a 12-well plate one day
215 before transfection. On the day of transfection, 2 μl siRNA (20 μM, Dharmacon, D-001810-10, L-012723-
216 00-0005, L-015791-00-0005) and 3 μl Lipofectamine RNAiMAX were diluted in 50 μl Opti-MEM
217 respectively and then mixed to incubate at room temperature for 15 min. Then, the complex was added
218 dropwise onto the cells. 24 h after transfection, medium was changed to DMEM/F12 supplement with 2%
219 charcoal stripped FBS. Decidualization was induced by the addition of 35 nM estradiol (Sigma, E1024), 1
220 μM medroxyprogesterone (Sigma, 1378001), and 0.05 mM cyclic adenosine monophosphate (Axxora,
221 JBS-NU-1502L) for 4 days with media changes every 48 hours.

222 **RNA Extraction and RT-qPCR**

223 For mRNA extraction from stromal cells, cells were lysed with TRIzol and processed using the DirectZol
224 kit (Zymo, R2051) following manufacturer's procedures. Approximately 100 ng of mRNA was reverse
225 transcribed into cDNA using iScript cDNA Supermix (Bio-Rad, 1708890) and amplified using specific
226 primers listed in Supplementary Table 1. Primers were amplified using 2X SYBR Green Reagent (Life
227 Technologies, 4364346) using a BioRad CFX384 Touch Real Time PCR Detection System. Data
228 analysis was performed by calculating ΔΔCT value towards the geometric mean of *GAPDH, ACTB* and
229 *RPL13A* and then normalized to siCTL. P-value was determined by One-Way ANOVA test with post hoc
230 Tukey test using GraphPad Prism. * $P \leq 0.05$, ** $P \leq 0.01$, *** $P \leq 0.001$, **** $P \leq 0.0001$.

231

232 **RESULTS**

233

234 **Generation of Mouse Models with Global HA-Tagged SMAD1 and PA-Tagged SMAD5 Proteins**

235 Activation of BMP signaling pathways has been established as one of the hallmarks of the
236 decidualization process[31,32]. Canonically, SMAD1/5 are regarded as downstream effectors of BMP2
237 signaling pathways to regulate decidual-specific gene expressions[6,33]. However, our recent findings
238 demonstrated that SMAD1/5 can also affect the sensitivity of the endometrium towards E2 and P4
239 stimulation[9]. Since we observed phenotypical differences between uterine-specific single SMAD1 and
240 single SMAD5 deletion mice, it is beneficial to delineate the role of SMAD1 and SMAD5 in mediating P4
241 responses during early pregnancy. We used CRISPR technology to generate genetically engineered
242 knock-in mice with an HA-tagged *Smad1* allele (herein called *Smad1*$^{HA/HA}$) and PA-tagged *Smad5* allele
243 (herein called *Smad5*$^{PA/PA}$) as shown in Figure 1A, B. The HA tag and the PA tag were inserted into the
244 N-terminus of the SMAD1 and SMAD5 proteins, respectively. Sanger sequencing was used to confirm
245 genomic insertion (Figure 1A, B). To validate the global detection of tagged proteins, we performed
246 immunoprecipitation followed by western blot analysis on different tissues from *Smad1*$^{HA/HA}$ and
247 *Smad5*$^{PA/PA}$ mice. We confirmed the HA and PA antibodies can readily detect HA-tagged SMAD1 and
248 PA-tagged SMAD5 proteins at the predicted size (Figure 1C, D). We also demonstrated the molecular
249 size and expression pattern of HA antibody detected SMAD1 protein was comparable to the SMAD1
250 antibody detected SMAD1 protein across different tissue types. Similarly, PA antibody showed
251 comparable signal intensity to the SMAD5 antibody in detecting SMAD5 protein across different tissue
252 types (Figure 1C, D). Thus, we successfully generated viable mouse models with global HA-tagged
253 SMAD1 and PA-tagged SMAD5 proteins.

254 **SMAD1 and SMAD5 Exhibit Shared and Unique Genomic Binding Sites During Decidualization**

255 The BMP signaling pathway regulates multiple key events during early pregnancy[5], mediated through
256 receptor-regulated SMAD proteins, including SMAD1 and SMAD5. As transducers of the BMP signaling
257 pathway, phosphorylated SMAD1 and SMAD5 form homomeric complexes and then couple with SMAD4
258 to assemble hetero-oligomeric complexes in the nucleus to execute transcription programs. Our previous
259 studies revealed that conditional ablation of SMAD1 and SMAD5 in the uterus decreased P4 response
260 during the peri-implantation period, suggesting that the transcriptional activities of PR depend on
261 BMP/SMAD1/5 signaling[9]. Furthermore, previous genome-wide PR binding studies show that SMAD1
262 and SMAD4 binding motifs are enriched in PR binding sites in the uterus[34].

263 To determine the shared and unique transcriptional regulomes of SMAD1 and SMAD5 contributing to the
264 diverse effects of BMP and P4 signaling pathways during decidualization, we first utilized Cleavage
265 Under Targets & Release Using Nuclease (CUT&RUN)[21] coupled with next generation sequencing to
266 profile genomic loci bound by SMAD1, SMAD5 and PR from mouse uterine tissues. We performed

267 CUT&RUN on the uterine tissues collected at 4.5 days post coitus (dpc), the time when the fertilized
268 embryo reaches the uterus physically and initiates the decidualization program[35] (Figure 2A). After
269 aligning CUT&RUN reads to the mm10 mouse genome, we called peaks using Sparse Enrichment
270 Analysis for CUT&RUN (SEACR)[22]. To identify high confidence peaks, background noise was
271 normalized to IgG and the stringent criteria for peak calling in SEACR was used. After merging common
272 peaks from two biological replicates, we identified 118,778 peaks for SMAD1 and 166,025 total peaks for
273 SMAD5. We visualized the enrichment of SMAD1 and SMAD5 peaks to the overall aligned chromatin
274 regions with clustering for preferential enrichment, as shown in Figure 2B. We found that 7.55% of
275 SMAD1 peaks and 9.53% of SMAD5 peaks were located within the ± 3 kb of the promoter regions
276 (Figure 2C, D). This corresponded to 10,368 genes that were directly bound by SMAD1 at the promoter
277 regions (± 3 kb), whereas 18,270 genes were directly bound by SMAD5 at the promoter regions (± 3 kb).
278 Among these, 4,933 genes were found in common between SMAD1 (47.5%) and SMAD5 (27.0%), while
279 2,744 and 7,427 genes were found to be uniquely bound by SMAD1 and SMAD5, respectively, providing
280 evidence for the shared and unique functions of SMAD1 and SMAD5 at the transcriptional level
281 (Supplement Figure 1B). Hence, interpreting how the binding events correlate to biological activity
282 requires comparisons with gene expression profiling in a tissue-specific manner.

283

284 **Identification of Direct Target Genes of SMAD1 and SMAD5 During Early Pregnancy**

285 To pinpoint the direct target genes of SMAD1 and SMAD5, we integrated transcriptomic data from
286 previously published[9] SMAD1/5 double conditional knockout mice using progesterone receptor cre
287 (SMAD1/5 cKO) (GSE152675) with SMAD1 and SMAD5 genomic data from this paper. We cross-
288 compared the differentially expressed genes in the transcriptomic data to the SMAD1 and SMAD5 bound
289 genes, respectively. Among the 805 significantly up-regulated genes, we identified 449 genes that were
290 both significantly up-regulated upon SMAD1/5 depletion and were directly bound by SMAD1 and
291 SMAD5, whereas 187 of the up-regulated genes were bound by SMAD5 only and 30 were bound only by
292 SMAD1 (Figure 3A). Among the 683 significantly down-regulated genes, we identified 523 genes that
293 were both significantly down-regulated upon SMAD1/5 depletion and were directly bound by SMAD1 and
294 SMAD5, whereas 83 of the down-regulated genes were bound by SMAD5 only and 13 were bound by
295 SMAD1 only (Figure 3B, Supplementary Table 2).

296 Next, we utilized Binding and Expression Target Analysis (BETA) algorithm[36] to perform motif enrichment
297 analysis of the direct target genes to identify putative co-factors working together with SMAD1 and
298 SMAD5 in controlling gene expression (Figure 3C,D, Supplement Files1,2). “Up-targets” represent genes
299 that were up-regulated in the SMAD1/5 cKO mouse uteri and showed either a SMAD1 or a SMAD5
300 binding site in the genomic profiling data. Similarly, “down-targets” represent genes that were down-

301 regulated in the SMAD1/5 cKO mouse uteri and displayed either a SMAD1 or a SMAD5 binding site.
302 Thus, motifs enriched in the "up-targets" indicate potential repressive SMAD1/5 co-factors while motifs
303 enriched in the "down-targets" indicate potential SMAD1/5 co-activators. Among the "up-targets" of
304 SMAD1, MYB Proto-Oncogene (*Myb*)/MYB Proto-Oncogene Like 1(*Mybl1*) motif was the most highly
305 enriched with a P-value of 1.85E-02. *Myb* and *Mybl1* transcription factors belong to MYB gene family,
306 which has been well-defined in controlling cell survival, proliferation and differentiation in cancer[37]. In
307 addition, they have also been reported to be E2 induced in human uterine leiomyoma samples[38].
308 Homeobox containing 1 (*Hmbox1*) and Krüppel-like factor (*Klf*) family members (*Klf4/Klf1/Klf12*) were
309 also identified as potential repressive co-factors of SMAD1 with P-values of 2.85E-02 and 3.75E-02
310 respectively (Figure 2C). Of note, *KLF4* has been reported to inhibit the binding activity of estrogen
311 receptor α (Erα) to estrogen response elements in promoter regions[39]. Among the "up-targets" of
312 SMAD5, EBF Transcription Factor 1 (*Ebf1*) motif was the most enriched with a P-Value of 1.57E-02.
313 Interestingly, *Ebf1* can directly repress the transcription of Forkhead box protein O1 (*Foxo1*)[40]. It is also
314 recognized as downstream effector of steroid hormone receptors in the mouse uterus[41]. Additionally,
315 motifs from transcription factors *Zfp128* and *Otx1* were also significantly enriched in the up-regulated
316 genes bound by SMAD5 (Figure 2D). Taken together, our enrichment analysis provided robust evidence
317 for identifying novel co-factors of SMAD1/5, and such co-regulating mechanisms are in line with the
318 unopposed E2 response observed in the SMAD1/5 cKO mice[9]. Furthermore, odd-skipped–related genes
319 (*Osr1* and *Osr2*) were identified as potential co-activators for SMAD1. *Osr2* has been reported to be
320 highly expressed in the human endometrium[42], and it was also abundantly detected at the protein level in
321 the human decidual tissues[43]. Decreased OSR2 level was observed in the patients with recurrent
322 spontaneous abortion and knockdown of *OSR2* impairs the decidualization process in the human
323 endometrial stromal cells[43]. Moreover, OSR1 has been reported to suppress BMP4 expression, which in
324 turn reduced the Wnt/β-catenin signaling pathways during lung development in xenopus[44]. Apart from
325 Osr family, motifs in the Homeobox genes (HOX) were found to be enriched in the "down-targets" from
326 both SMAD1 and SMAD5 datasets. Specifically, *Hoxa11/Hoxd12/Hoxc10* were predicted to be co-
327 activators for SMAD1 while *Hoxd10* was indicated to be closely interacting with SMAD5. Indeed, HOX
328 genes are critical for endometrial development in normal and disease conditions and are essential during
329 the establishment of pregnancy[45-48].

330 With direct target genes of SMAD1 and SMAD5 identified, we then analyzed the Gene Ontology
331 enrichment for the SMAD1/5 shared up-targets and down-targets, respectively. We found that "up-
332 targets" genes exhibit enrichment for regulation of cell-cell adhesion, cell junction organization and
333 desmosomes organization (Figure 3E, Supplementary Table 3). Moreover, among the "down-targets"
334 genes, we found the enrichment for blood vessel / vasculature development and extracellular matrix
335 organization categories (Figure 3F, Supplementary Table 4). Indeed, during early pregnancy, the

336 stimulation from corpus-luteum derived P4 enabled the endometrium to be transformed to a receptive
337 state, which allows subsequent embryo attachment and develop through the epithelium into the stromal
338 sections[31]. During this process, apportioned direct cell-cell contacts are ensured by tight and adherent
339 junctions and such interactions are key in facilitating implantation and embryo invasion. In accordance
340 with our findings, desmosomes and adherens junctions were extensively described to decline in the early
341 pregnancy period, which facilitates the invasion of trophoblast through the epithelial layer[49-52]. In addition,
342 the stromal compartment of the endometrium also undergoes profound vascular remodeling. Precise
343 regulations of angiogenesis are required to establish an extensive vascular network, which is essential to
344 ensure blood supply and successful embryonic development[53,54]. Collectively, our findings present
345 evidence that emphasizes the shared roles of SMAD1 and SMAD5 in facilitating endometrial transitions
346 during early pregnancy.

347 **Direct Target Genes of SMAD1 and SMAD5 Maintain the Homeostasis of Uterine Function**

348 To discover novel direct target genes of SMAD1/5, we visualized key genes of interest from the up-
349 targets and down-targets. As shown in Figure 4A, data from RNA-seq represents the decrease of several
350 "down-targets" in the SMAD1/5 cKO mouse uteri, including Retinoic Acid-Related Orphan Receptor B
351 (*Rorb*), Follistatin (*Fst*), Lymphoid Enhancer Binding Factor 1 (*Lef1*), and Insulin Like Growth Factor 1
352 (*Igf1*). Integrative Genomics Viewer (IGV) track view shows the exemplary SMAD1/5 binding activities
353 near the promoter regions of *Rorb* and *Fst* Figure 4B, demonstrating that these genes are bona fide
354 direct target genes of SMAD1/5. *Rorb* belongs to the nuclear receptor families in the retinoic acid (RA)
355 signaling pathways[55] and is considered as a marker for mesenchymal progenitor cells in the stroma
356 compartment of the endometrium[56]. In murine models, deficient RA signaling through the perturbation of
357 RA receptor in the uterus leads to implantation and decidualization failure[57]. *Fst* binds several TGFβ
358 family ligands and thereby inhibits TGFβ family signaling extracellularly[58]. Under physiological conditions,
359 *Fst* is up-regulated in the decidua during early pregnancy. Conditional deletion of *Fst* in the mouse uterus
360 results in severe subfertility with a phenotype of non-receptive epithelium and poor-differentiated
361 stroma[59]. Notably, RA signaling deficiency also decreases *Fst* levels in the uterus and systematic
362 administration of FST can fully rescue the deficient-decidualization phenotype but not the non-receptive
363 phenotype observed in the RA receptor mutant mice[57]. Our results suggest a direct relationship between
364 BMP and RA signaling pathway, accomplished by SMAD1/5 at the transcriptional level, likely
365 establishing a positive signaling feedback loop. Apart from being a crucial transcriptional activator,
366 SMAD1/5 also plays a role in repressing key gene expression pathways. Shown in Figure 4C, upon the
367 deletion of SMAD1/5 in the mouse uteri, several E2-responsive genes were significantly up-regulated,
368 including Fibroblast Growth Factor Receptor 2 (*Fgfr2*), Matrix Metallopeptidase 7 (*Mmp7*) and Wnt
369 Family Member 7B (*Wnt7b*). In addition, *Inhbb*, a downstream target of *Fst*[59], is also a target gene of
370 SMAD1/5 that resulted in transcriptional repression. SMAD1/5 binding on the *Fgfr2* and *Mmp7* genes are

371 exemplified in an IGV track view in Figure 4D. *Fgfr2* and its ligands regulate epithelial cell proliferation
372 and differentiation. Components of the Fibroblast Growth Factor (*Fgf*) signaling pathway are cyclically
373 expressed in the uterus and act as paracrine and/or autocrine mediators of epithelial-stromal
374 interactions[60,61]. During early pregnancy in mice, P4 inhibits expression of *Fgf2* in the stromal cells, which
375 is critical to counteract the E2-driven epithelial proliferation[60]. Similar observations are reported in gilts,
376 where the expression of *Fgfr2* decreased alongside with increased parity of the sows[62]. It is also
377 noteworthy that loss of function of *Fgfr2* in the mouse uterus leads to luminal epithelial stratification and
378 peri-implantation pregnancy loss[61]. Moreover, *Mmp7* and *Wnt7b* are up-regulated upon E2 stimulation
379 and participate in the re-epithelialization of the endometrium and implantation process, respectively[63-65].
380 In accordance with the phenotype of hyperproliferative endometrial epithelium during early pregnancy
381 observed SMAD1/5 cKO mice, we demonstrated that the suppression of key E2-responsive genes, such
382 as *Fgfr2* and *Mmp7,* by SMAD1/5 maintains the precise balance between E2 and P4.

383 To explore the major cell types regulated by SMAD1/5 direct targets in human, we profiled the
384 expression levels of the key "up-targets" and "down-targets" in the different cell types of the human
385 endometrium. Using previously published single-cell RNA seq data of human endometrium[66], we
386 visualized the expression patterns of suppressive targets and activating targets of SMAD1/5 (Figure 4E).
387 Apart from the major epithelial and stromal compartments, SMAD1/5 target genes are also widely
388 expressed in the immune cell populations. Such observation reinforced the importance of the BMP
389 signaling pathways in establishing an immune-privileged environment at the maternal-fetal interface[67].

390 **SMAD1 and SMAD5 Co-regulate PR Target Genes**

391 SMAD1/5 cKO mice were infertile due to endometrial defects and displayed decreased P4 response
392 during the peri-implantation period[9]. Hence, we hypothesized that SMAD1 and SMAD5 act as co-
393 regulators of P4-responsive genes during the window of implantation and are required for endometrial
394 receptivity and decidualization. By determining the genomic co-occupancy of SMAD1, SMAD5 and PR,
395 we aimed to clarify the transcriptional interplay between the BMP and P4 signaling pathways. To this
396 end, we performed additional PR CUT&RUN experiments on the uteri of mice collected at 4.5 dpc and
397 identified 134,737 peaks showing PR binding activities (Figure 5A). We identified 7,393 genes that were
398 directly bound by PR at the promoter regions (± 3 kb), among which, 2596 genes were also concurrently
399 bound by both SMAD1 and SMAD5 at the promoter regions (± 3 kb) (Supplement Figure 1B).

400 Next, we performed KEGG pathway enrichment for the genes co-bound by SMAD1, SMAD5 and PR. As
401 expected, pathways critical for decidualization such as relaxin signaling pathways and WNT signaling
402 cascade were identified in the enrichment results (Figure 5B, Supplementary Table 5). We visualized
403 exemplary genes co-regulated by SMAD1, SMAD5 and PR and presented in the normalized IGV track
404 view (Figure 5C). We demonstrated SMAD1, SMAD5 and PR showed co-occupancy at the loci of the

405 SRY-Box Transcription Factor 17 (*Sox17*), Inhibitor of DNA binding 2 (*Id2*), Forkhead box protein O1
406 (*Foxo1*), Insulin-like growth factor 1 (*Igf1*), Transforming growth factor beta receptor 2 (*Tgfbr2*) and
407 RUNX family transcription factor 1 (*Runx1*) (Figure 5C). *Sox17* has been reported as one of the direct
408 target genes of PR[34] and is essential for uterine functions during implantation and early pregnancy[68,69].
409 More recent studies also showed the importance of *Sox17* in regulating uterine epithelial–stromal
410 crosstalk and its indispensable role in female fertility[70]. We provided evidence that *Sox17* is also directly
411 regulated by SMAD1/5 complexes. Our results indicated that *Id2*, considered as canonical direct
412 transcriptional targets of BMP-SMAD signaling[71,72] is also regulated by PR. We also confirmed that
413 known P4-responsive genes such as *Tgfbr2*[73] and *Runx1*[74], as well as decidual markers such as *Foxo1*[75]
414 and *Igf1*[76], were co-regulated by SMAD1, SMAD5 and PR (Figure 5C).

415 To identify additional transcription factors that are associated with the regulatory interplay between
416 SMAD1/5 and PR during decidualization, we performed unbiased motif analysis on the shared
417 CUT&RUN peaks between SMAD1/5 and PR. We reported the top 10 transcription factors harboring the
418 enriched motifs, including NANOG, Homeobox A protein family (HOXA11 and HOXA9), NK6 homeobox
419 1(NKX6.1), TGFB induced factor homeobox 2 (TGIF2), FOS, RUNX family transcription factor 2
420 (RUNX2), Androgen receptor (AR), SOX17 and Lymphoid enhancer-binding factor 1 (LEF1) (Figure 5D,
421 Supplementary Table 6). Many of these putative interactors have been reported to interact with the
422 SMAD proteins in other biological processes. For example, NANOG interacts with SMAD1 during
423 mesoderm differentiation[77]. HOXA9 forms heterodimers with SMAD4, leading to BMP-driven initiation of
424 transcription from the mouse *Opn* promoter *in vitro*[78,79]. Transcription factor AP-1 family (FOS) and
425 RUNX2, as well as β-catenin/Lef1 complex, increase the effectiveness and specificity of DNA binding
426 activities of SMAD1/5 in response to BMP ligand stimuli[80-82]. To further evaluate the key roles of
427 SMAD1/5 as major uterine transcription regulators, we cross-compared the genomic binding sites of
428 SMAD1/5 with known key transcription factors, namely aforementioned SOX17 (Supplement Figure 1E,
429 Supplementary Table 7), as well as NR2F2 (Supplement Figure 1F, Supplementary Table 8), an
430 essential regulator of hormonal response[83], using our CUT&RUN data sets and published mouse uterine
431 SOX17 and NR2F2 ChIP-seq data sets (GSE118328, GSE232583). Among the annotated genes, 5402
432 genes are shared between SMAD1/5 and SOX17, and 1922 genes are shared between SMAD1/5 and
433 NR2F2. Such observations indicate a potential co-regulatory mechanism between SMAD1/5 and other
434 key uterine transcription factors in maintaining appropriate uterine functions. Overall, our analyses
435 demonstrate that the transcriptional activity of SMAD1, SMAD5, and PR coordinate the expression of key
436 genes required for endometrial receptivity and decidualization.

437 **Decidualization of Human Endometrial Stromal Cells Requires SMAD1/SMAD5**

438 We next sought to functionally characterize the role of SMAD1/5 during decidualization in human
439 endometrial stromal cells. To do so, we examined the effect of SMAD1/5 perturbations on the
440 decidualization of primary human endometrial stromal cells (EnSCs). EnSCs were transfected with short
441 interfering RNAs (siRNAs) targeting each gene (*SMAD1* and *SMAD5)* and subjected to *in vitro*
442 decidualization by treatment with E2-cAMP-and MPA (EPC) for 4.5 days (Figure 6A). We hypothesized
443 that the combined SMAD1/5 knockdown would impair the decidualization process significantly compared
444 to cells treated with non-targeting siRNAs. Our results demonstrated that SMAD1/5 knockdown affected
445 decidualization and led to significantly decreased expression of the canonical decidual markers, *PRL and*
446 *IGFBP1* in EnSCs (Figure 6B). The PR co-regulator, *FOXO1*[84]*,* also exhibited a significant decreasing
447 trend in the siSMAD1/5 group. We also examined the expression level of the RA pathway regulator gene,
448 *RORB*, and of the SMAD4-PR target gene, *KLF15*[12], following SMAD1/5 perturbation. We observed a
449 significant decrease in both *RORB* and *KLF15* expression upon SMAD1/5 knockdown during *in vitro*
450 decidualization treatment (Figure 6C). Taken together, our findings indicate SMAD1/5 can modulate PR
451 activity during decidualization and that this transcriptional cooperation is required for the *in vitro*
452 decidualization of primary human endometrial stromal cells.

453 **DISCUSSION**

454 SMAD proteins are canonical transcription factors that are activated in response to TGFβ family signaling
455 and mediate the biological effects of these pathophysiologically critical ligands[81]. While SMAD2 and
456 SMAD3 are downstream of TGFβs, activins, and multiple other family ligands, SMAD1 and SMAD5
457 preferentially transduce BMP signaling pathways and are regarded as pivotal activators for many
458 physiological processes, including bone development, cardiac conduction system development, and
459 embryonic pattern specification[85-87]. Importantly, SMAD1 and SMAD5 are implicated in diverse female
460 reproductive physiology and pathophysiology processes[5,9,88-90].

461 Due to high structural similarity, SMAD1/5 have been suggested to be redundant from the studies in
462 ovarian biology and chondrogenesis[89,91]. However, other studies clearly demonstrated that SMAD1/5
463 have different roles in governing hematopoiesis and uterine functions[9,92]. The DNA binding activities of
464 SMAD1 and SMAD5 have not been readily distinguished from each other due to anti-phospho antibody
465 limitations. To robustly define the roles of SMAD1/5 in regulating transcriptional programs *in vivo*, we
466 produced two genetically engineered mouse models with global knock-in of an HA tag and a PA tag in
467 the *Smad1* and *Smad5* loci, respectively. We showed that SMAD1 and SMAD5 not only have shared
468 transcriptional activities but also have unique roles in uterine physiology. In agreement with previous
469 studies showing that SMAD1/5 function is partially redundant[89,91], we confirmed that SMAD1/5 share a
470 total of 972 direct target genes in the uterus. Furthermore, we demonstrated that 43 genes were uniquely
471 regulated by SMAD1 whereas 270 genes are specifically regulated by SMAD5 only. Our motif analysis

472 also revealed distinct potential co-factors between SMAD1 and SMAD5, providing evidence at the
473 molecular level to mechanistically delineating the distinct roles of SMAD1 and SMAD5 in directing
474 cellular processes in the uterus.

475 Apart from directly regulating target gene expression, our data demonstrate that SMAD1/5 present as
476 dense genomic occupancies. To date, only a limited amount of transcription factors have been
477 investigated using the CUT&RUN-seq technique from the tissue samples due to antibody compatibility
478 issue. We recognize that the binding sites and gene number identified here are quite high; however, the
479 high density of binding events was also observed in the ENCODE[93] chromatin immunoprecipitation
480 followed by sequencing (ChIP-seq) data for SMAD1 and SMAD5 in the human K562 cells, detecting an
481 average of 63,563 peaks for SMAD1 and 109,682 peaks for SMAD5. (Data accessed through GSE95876
482 and GSE127365 from Gene Expression Omnibus). Multiple aspects can contribute to the observation of
483 dense SMAD1/5 genome occupancies. First, transcription factors (TFs) tend to dwell or "search and
484 bind" throughout the genome[94]. Such events may not yield actual biological effects but rather are due to
485 differences in motif binding affinities[95]. Second, apart from robust binding activities, TFs may not initiate
486 transcription programs owing to the lack of co-factors or favorable conditions to exert their functions[96].
487 Additionally, TF binding sites and target genes are unlikely to have a one-to-one relationship. TFs could
488 be positioned from the proximal promoter regions to hundreds of kilobases afar to modulate gene
489 expression. In the meantime, the same binding site could regulate multiple genes by interacting with
490 different promoters in different subpopulations of cells. Lastly, TFs usually direct target gene expression
491 in a cell-type specific manner[97]. Our genomic profiling samples were collected from whole uterus at the
492 time of 4.5 dpc, containing a great range of cell populations, including but not limited to the epithelium
493 (luminal and glandular), stroma (progenitors and differentiated cells), myometrium, endothelium, and
494 immune cell populations. The data is therefore expected to depict the dynamic and complex activities of
495 SMAD1/5 in the entire uterus. Together, the stringent filtering and normalization criteria, comparable
496 peak number to the published dataset and IGV track view visualization collectively validate our
497 CUT&RUN experiments and uncover the enriched regions as robust SMAD1/5 binding events. Our
498 studies also examined the role of SMAD1/5 in mediating progesterone responses at the genomic and
499 transcription levels. Similarly, our analysis was based on data sets generated from the whole mouse
500 uterus, which contains multiple compartments of the uterine structures, including but not limited to
501 epithelium and stroma. Published studies have shown that nuclear SMAD1/5 localize to the stroma and
502 epithelium during the decidualization process at 4.5 dpc, during the window of implantation[9]. Conditional
503 deletion of SMAD1/5 exclusively in the uterine epithelium using lactoferrin-icre (*Ltf*-icre) results in severe
504 subfertility due to impaired implantation and decidual development[98]. Conditional deletion of SMAD1/5/4
505 exclusively in the cells from mesenchymal lineage (including uterine stroma) using anti-Mullerian
506 hormone type 2 receptor cre (*Amhr2-cre*) results in infertility with defective decidualization[89,90]. Given the

507 essential roles of SMAD1/5 in both stroma and epithelium identified by previous studies, we believe that
508 the transcriptional co-regulatory roles of SMAD1/5 and PR reported here using the whole uterus
509 validates a relationship between SMAD1/5 and PR in both the stromal and epithelial compartments.
510 However, it does not rule out potential co-regulatory roles of SMAD1/5 and PR in the myometrium,
511 immune cells, and/or endothelium, given that whole uterus was used. The specific transcriptional
512 evaluations of SMAD1/5 in the stroma versus the epithelium would require future single-cell sequencing
513 (i.e., digital cytometry[99]) and/or spatial transcriptomic analysis.

514 Although our studies herein confirm that SMAD1 and SMAD5 proteins have distinct transcriptional
515 regulatory activities, our previous studies demonstrated that while SMAD5 can functionally replace
516 SMAD1, SMAD1 cannot replace SMAD5 in the uterus[9]. How this epistatic relationship is established in a
517 tissue-specific manner still needs to be determined by further biochemical investigations. In addition,
518 further studies are needed to uncover whether SMAD1 and SMAD5 response differently upon ligand
519 stimulation in the uterus, and if so, how the preference is achieved. Our study provides versatile *in vivo*
520 genetic tools for these questions and can advance the toolbox for the field studying BMP signaling
521 pathways. Because our mouse models are global knock-in mice, they will not only serve as a powerful
522 tool for studying BMP signaling pathways in the reproductive system but will also promote the study of
523 BMP signaling in other organs and tissues.

524 BMP signaling pathways are involved in a plethora of cellular processes and appropriate functioning of
525 the BMP pathway depends on the precise crosstalk with other signaling pathways. Coordinated
526 communication with other pathways can yield synergistic effects and lead to a complex regulatory
527 network of biological processes. To be specific, SMAD1/5 mediates the crosstalk with the WNT/β-catenin
528 pathway. WNT signaling inhibits glycogen synthase kinase 3β (GSK3β) activity and prevents SMAD1
529 from degradation which governs the embryonic pattern formation[100]. Also, SMAD1/5 can physically
530 interact with T-cell factor (TCF) or lymphoid enhancer factor (LEF) transcription factors to form
531 transcriptional complexes to activate the transcription of many WNT-and BMP-responsive genes[101]. In
532 addition, SMAD1 and SMAD5 can directly associate with Notch intracellular domain and enhance known
533 Notch target gene expression by binding to their regulatory DNA sequences[102]. Intriguingly, in prostate
534 cells, SMAD1 physically interacts with the androgen receptor (AR) and halts the androgen-stimulated
535 prostate cell growth[103]. Moreover, we provide first-hand evidence showing that BMP signaling pathways
536 converge with RA signaling pathways through the regulation of RORB by SMAD1/5. Further studies will
537 grant a more detailed mechanism of the positive feedback loop between BMP and RA signaling.

538 Our previous studies suggest that the mouse endometrium presents decreased P4 responsiveness
539 following the conditional deletion of SMAD1/5 in the uterus[9]. In accordance with the phenotypical

540 observation, we offer compelling support in our current study that SMAD1/5 work collectively with PR to
541 regulate their target genes and that SMAD1/5 mediate the crosstalk between BMP and P4 signaling
542 pathways during decidualization, a key process to ensure a successful pregnancy, and ultimately direct
543 the biological transformations of the uterus during early pregnancy. We provide genomic evidence that
544 SMAD1/5 are co-bound at around 35% of PR target genes in the mouse uterus during decidualization.
545 Correspondingly, in a previously published study where they performed PR ChIP-seq in the mouse
546 uterus after P4 stimulation, the SMAD1 motif was the 5th most significantly enriched sequence motifs
547 identified[34]. In parallel, we also identified nuclear receptor motifs (i.e., PR sequence motifs) enriched in
548 the SMAD1/5 binding sites (Supplement Figure 1C,D). From pathway enrichment analysis, we
549 demonstrate that genes with SMAD1/5 and PR bound at the promoter regions are enriched for key
550 pathways in directing the decidualization process, such as WNT and relaxin signaling pathways. Future
551 studies can benefit from analyzing binding events beyond the promoter regions. Profiling the PR genome
552 occupancy in the SMAD1/5 deficient mice would provide an interesting perspective to reevaluate the
553 major regulatory roles of SMAD1/5 in mediating uterine transcriptomes. In this study, we determined the
554 overlapped transcriptional control between SMAD1/5 and PR at the gene level, and functionally validated
555 the regulatory effect at the transcript level in a human stromal cell decidualization model. While we
556 observe a subset of peak representations that do not overlap at the base pair level in the promoter
557 regions, future functional screenings at the promoter level, such as luciferase reporter assays to assess
558 transcriptional co-activation by SMAD1/5 and PR, will advance this study.

559 SMADs are known to recruit co-repressors (*i.e.*, Ski[104]) or co-activators (*i.e.*, p300[105]) to inhibit or activate
560 target gene transcription, less is known about their cell-specific co-factors that confer the precise spatial-
561 temporal control over binding activities to target genes. Our study highlights the potential co-factors by
562 integrating both genomic and transcriptomic data to delineate signaling crosstalks that are responsible for
563 maintaining tissue homeostasis, especially in the female reproductive tract.

564 Since mice only undergo decidualization upon embryo implantation whilst human stromal cells undergo
565 cyclic decidualization in each menstrual cycle in response to rising levels of progesterone[35],
566 asynchronous gene responses may occur in comparison between mouse models and human cells.
567 However, cellular transformation during decidualization is conserved between mice and humans[31], which
568 makes findings in the mouse models a valuable and transferable resource to be evaluated in human
569 tissues. Accordingly, our functional validation studies were performed using human endometrial stromal
570 cells induced to decidualize *in vitro* for four days, which models the early phases of decidualization.
571 Additional transcriptomic studies of the SMAD1/5 perturbations in human endometrial stromal cells will
572 be of great resource in understanding the entire SMAD1/5 regulomes in humans.

573 In summary, our findings and those of others indicate that SMAD1 and SMAD5 not only are signal
574 transducers for BMP signaling pathways, but also engage extensively in the crosstalk with PR signaling
575 pathways. While P4 responses are critical for early pregnancy establishment, abnormal P4 responses
576 are implicated in diseases such as endometriosis and endometrial cancers[106-109]. Hence, our results
577 which show that BMP and P4 signaling pathways synergize within the endometrium; these key pathways
578 can shed light on the endometrial contribution to conditions that impact reproductive health in women,
579 including early pregnancy loss, endometriosis, and endometrial cancer. Furthermore, we anticipate that
580 the SMAD1/5 knock-in tagged transgenic mouse models developed herein will be useful for studying
581 BMP/SMAD1/5 signaling pathways in other reproductive and non-reproductive tract tissues in the body.

582

583

584 **DATA AVAILABILITY**

585 Sequencing data and analyses are deposited in the Gene Expression Omnibus under accession number
586 GSE237975. (Reviewer token: gludeooirhczxcj)
587

588 **SUPPLEMENTARY DATA**

589 Supplementary Table 1: DNA sequences used in the study.
590 Supplementary Table 2: Direct target genes of SMAD1/5.
591 Supplementary Table 3: Results of Gene Ontology enrichment analysis of shared direct target genes of
592 SMAD1/5 from the up-targets.
593 Supplementary Table 4: Results of Gene Ontology enrichment analysis of shared direct target genes of
594 SMAD1/5 from the down-targets.
595 Supplementary Table 5: Results of KEGG pathway enrichment analysis for shared genes bound by
596 SMAD1, SMAD5, and PR.
597 Supplementary Table 6: Results of motif analysis results for shared peaks between SMAD1, SMAD5 and
598 PR.
599 Supplementary Table 7: Gene overlapping results of SMAD1/5 and SOX17.
600 Supplementary Table 8: Gene overlapping results of SMAD1/5 and NR2F2.
601 Supplementary File 1: Complete list of motif enrichment analysis from the up-targets and down-targets
602 for SMAD1.
603 Supplementary File 2: Complete list of motif enrichment analysis from the up-targets and down-targets
604 for SMAD5.

Supplementary Figures: Supplementary Figures 1-3

AUTHOR CONTRIBUTIONS

Zian Liao: Conceptualization, Formal analysis, Methodology, Validation, Writing—original draft. Suni Tang: Data curation, Investigation, Methodology, Visualization, Writing—review & editing. Kaori Nozawa: Data curation, Investigation, Methodology, Writing—review & editing. Keisuke Shimada: Data curation, Methodology, Writing—review & editing. Masahito Ikawa: Project administration, Resources. Diana Monsivais: Conceptualization, Investigation, Supervision, Funding acquisition, Writing – review & editing. Martin M. Matzuk: Conceptualization, Supervision, Funding acquisition, Writing – review & editing.

ACKNOWLEDGEMENTS

FUNDING

This research is supported by Eunice Kennedy Shriver National Institute of Child Health and Human Development grants HD105800 (D.M.), HD096057 (D.M.), HD032067 (M.M.M.), and HD110038 (M.M.M.). DM is supported by a Next Gen Pregnancy Award from the Burroughs Wellcome Fund (NGP10125).

CONFLICT OF INTEREST

No conflict of interest is declared by the authors.

REFERENCE

BIBLIOGRAPHY AND REFERENCES

1 Boivin, J., Bunting, L., Collins, J. A. & Nygren, K. G. International estimates of infertility prevalence and treatment-seeking: potential need and demand for infertility medical care. *Hum Reprod* **22**, 1506-1512, doi:10.1093/humrep/dem046 (2007).

2 Martinez, G. M., Daniels, K. & Febo-Vazquez, I. Fertility of Men and Women Aged 15-44 in the United States: National Survey of Family Growth, 2011-2015. *Natl Health Stat Report*, 1-17 (2018).

3 Wang, X. *et al.* Conception, early pregnancy loss, and time to clinical pregnancy: a population-based prospective study. *Fertil Steril* **79**, 577-584, doi:10.1016/s0015-0282(02)04694-0 (2003).

4 Chang, H., Brown, C. W. & Matzuk, M. M. Genetic analysis of the mammalian transforming growth factor-beta superfamily. *Endocr Rev* **23**, 787-823, doi:10.1210/er.2002-0003 (2002).

640 5 Monsivais, D., Matzuk, M. M. & Pangas, S. A. The TGF-beta Family in the Reproductive Tract.
641 *Cold Spring Harb Perspect Biol* **9**, doi:10.1101/cshperspect.a022251 (2017).
642 6 Lee, K. Y. *et al.* Bmp2 is critical for the murine uterine decidual response. *Mol Cell Biol* **27**, 5468-
643 5478, doi:10.1128/MCB.00342-07 (2007).
644 7 Monsivais, D. *et al.* BMP7 Induces Uterine Receptivity and Blastocyst Attachment. *Endocrinology*
645 **158**, 979-992, doi:10.1210/en.2016-1629 (2017).
646 8 Nagashima, T. *et al.* BMPR2 is required for postimplantation uterine function and pregnancy
647 maintenance. *J Clin Invest* **123**, 2539-2550, doi:10.1172/JCI65710 (2013).
648 9 Monsivais, D. *et al.* Endometrial receptivity and implantation require uterine BMP signaling
649 through an ACVR2A-SMAD1/SMAD5 axis. *Nat Commun* **12**, 3386, doi:10.1038/s41467-021-
650 23571-5 (2021).
651 10 Matzuk, M. M., Kumar, T. R. & Bradley, A. Different phenotypes for mice deficient in either
652 activins or activin receptor type II. *Nature* **374**, 356-360, doi:10.1038/374356a0 (1995).
653 11 Clementi, C. *et al.* Activin-like kinase 2 functions in peri-implantation uterine signaling in mice and
654 humans. *PLoS Genet* **9**, e1003863, doi:10.1371/journal.pgen.1003863 (2013).
655 12 Monsivais, D. *et al.* Uterine ALK3 is essential during the window of implantation. *Proc Natl Acad*
656 *Sci U S A* **113**, E387-395, doi:10.1073/pnas.1523758113 (2016).
657 13 Teklenburg, G. *et al.* Natural selection of human embryos: decidualizing endometrial stromal cells
658 serve as sensors of embryo quality upon implantation. *PLoS One* **5**, e10258,
659 doi:10.1371/journal.pone.0010258 (2010).
660 14 Brosens, J. J. *et al.* Uterine selection of human embryos at implantation. *Sci Rep* **4**, 3894,
661 doi:10.1038/srep03894 (2014).
662 15 Weimar, C. H. *et al.* Endometrial stromal cells of women with recurrent miscarriage fail to
663 discriminate between high- and low-quality human embryos. *PLoS One* **7**, e41424,
664 doi:10.1371/journal.pone.0041424 (2012).
665 16 Salker, M. S. *et al.* Deregulation of the serum- and glucocorticoid-inducible kinase SGK1 in the
666 endometrium causes reproductive failure. *Nat Med* **17**, 1509-1513, doi:10.1038/nm.2498 (2011).
667 17 Garrido-Gomez, T. *et al.* Defective decidualization during and after severe preeclampsia reveals
668 a possible maternal contribution to the etiology. *Proc Natl Acad Sci U S A* **114**, E8468-E8477,
669 doi:10.1073/pnas.1706546114 (2017).
670 18 Garrido-Gomez, T. *et al.* Preeclampsia: a defect in decidualization is associated with deficiency of
671 Annexin A2. *Am J Obstet Gynecol* **222**, 376 e371-376 e317, doi:10.1016/j.ajog.2019.11.1250
672 (2020).
673 19 Shimada, K. *et al.* ARMC12 regulates spatiotemporal mitochondrial dynamics during
674 spermiogenesis and is required for male fertility. *Proc Natl Acad Sci U S A* **118**,
675 doi:10.1073/pnas.2018355118 (2021).
676 20 Fang, B. *et al.* Circadian enhancers coordinate multiple phases of rhythmic gene transcription in
677 vivo. *Cell* **159**, 1140-1152, doi:10.1016/j.cell.2014.10.022 (2014).
678 21 Skene, P. J. & Henikoff, S. An efficient targeted nuclease strategy for high-resolution mapping of
679 DNA binding sites. *Elife* **6**, doi:10.7554/eLife.21856 (2017).
680 22 Meers, M. P., Tenenbaum, D. & Henikoff, S. Peak calling by Sparse Enrichment Analysis for
681 CUT&RUN chromatin profiling. *Epigenetics Chromatin* **12**, 42, doi:10.1186/s13072-019-0287-4
682 (2019).
683 23 Kent, W. J., Zweig, A. S., Barber, G., Hinrichs, A. S. & Karolchik, D. BigWig and BigBed: enabling
684 browsing of large distributed datasets. *Bioinformatics* **26**, 2204-2207,
685 doi:10.1093/bioinformatics/btq351 (2010).
686 24 Heinz, S. *et al.* Simple combinations of lineage-determining transcription factors prime cis-
687 regulatory elements required for macrophage and B cell identities. *Mol Cell* **38**, 576-589,
688 doi:10.1016/j.molcel.2010.05.004 (2010).
689 25 Yu, G., Wang, L. G. & He, Q. Y. ChIPseeker: an R/Bioconductor package for ChIP peak
690 annotation, comparison and visualization. *Bioinformatics* **31**, 2382-2383,
691 doi:10.1093/bioinformatics/btv145 (2015).

26 Ramirez, F. *et al.* deepTools2: a next generation web server for deep-sequencing data analysis. *Nucleic Acids Res* **44**, W160-165, doi:10.1093/nar/gkw257 (2016).
27 Initiative, C. Z. (2023).
28 Warren, L. A. *et al.* Analysis of menstrual effluent: diagnostic potential for endometriosis. *Mol Med* **24**, 1, doi:10.1186/s10020-018-0009-6 (2018).
29 Nayyar, A. *et al.* Menstrual Effluent Provides a Novel Diagnostic Window on the Pathogenesis of Endometriosis. *Front Reprod Health* **2**, 3, doi:10.3389/frph.2020.00003 (2020).
30 Martinez-Aguilar, R. *et al.* Menstrual blood-derived stromal cells modulate functional properties of mouse and human macrophages. *Sci Rep* **10**, 21389, doi:10.1038/s41598-020-78423-x (2020).
31 Gellersen, B. & Brosens, J. J. Cyclic decidualization of the human endometrium in reproductive health and failure. *Endocr Rev* **35**, 851-905, doi:10.1210/er.2014-1045 (2014).
32 Magro-Lopez, E. & Munoz-Fernandez, M. A. The Role of BMP Signaling in Female Reproductive System Development and Function. *Int J Mol Sci* **22**, doi:10.3390/ijms222111927 (2021).
33 Li, Q. *et al.* Bone morphogenetic protein 2 functions via a conserved signaling pathway involving Wnt4 to regulate uterine decidualization in the mouse and the human. *J Biol Chem* **282**, 31725-31732, doi:10.1074/jbc.M704723200 (2007).
34 Rubel, C. A. *et al.* Research resource: Genome-wide profiling of progesterone receptor binding in the mouse uterus. *Mol Endocrinol* **26**, 1428-1442, doi:10.1210/me.2011-1355 (2012).
35 Ramathal, C. Y., Bagchi, I. C., Taylor, R. N. & Bagchi, M. K. Endometrial decidualization: of mice and men. *Semin Reprod Med* **28**, 17-26, doi:10.1055/s-0029-1242989 (2010).
36 Wang, S. *et al.* Target analysis by integration of transcriptome and ChIP-seq data with BETA. *Nat Protoc* **8**, 2502-2515, doi:10.1038/nprot.2013.150 (2013).
37 Ciciro, Y. & Sala, A. MYB oncoproteins: emerging players and potential therapeutic targets in human cancer. *Oncogenesis* **10**, 19, doi:10.1038/s41389-021-00309-y (2021).
38 Swartz, C. D., Afshari, C. A., Yu, L., Hall, K. E. & Dixon, D. Estrogen-induced changes in IGF-I, Myb family and MAP kinase pathway genes in human uterine leiomyoma and normal uterine smooth muscle cell lines. *Mol Hum Reprod* **11**, 441-450, doi:10.1093/molehr/gah174 (2005).
39 Akaogi, K. *et al.* KLF4 suppresses estrogen-dependent breast cancer growth by inhibiting the transcriptional activity of ERalpha. *Oncogene* **28**, 2894-2902, doi:10.1038/onc.2009.151 (2009).
40 Timblin, G. A. & Schlissel, M. S. Ebf1 and c-Myb repress rag transcription downstream of Stat5 during early B cell development. *J Immunol* **191**, 4676-4687, doi:10.4049/jimmunol.1301675 (2013).
41 Pan, H., Zhu, L., Deng, Y. & Pollard, J. W. Microarray analysis of uterine epithelial gene expression during the implantation window in the mouse. *Endocrinology* **147**, 4904-4916, doi:10.1210/en.2006-0140 (2006).
42 Fagerberg, L. *et al.* Analysis of the human tissue-specific expression by genome-wide integration of transcriptomics and antibody-based proteomics. *Mol Cell Proteomics* **13**, 397-406, doi:10.1074/mcp.M113.035600 (2014).
43 Ma, W. *et al.* MAX deficiency impairs human endometrial decidualization through down-regulating OSR2 in women with recurrent spontaneous abortion. *Cell Tissue Res* **388**, 453-469, doi:10.1007/s00441-022-03579-z (2022).
44 Rankin, S. A., Gallas, A. L., Neto, A., Gomez-Skarmeta, J. L. & Zorn, A. M. Suppression of Bmp4 signaling by the zinc-finger repressors Osr1 and Osr2 is required for Wnt/beta-catenin-mediated lung specification in Xenopus. *Development* **139**, 3010-3020, doi:10.1242/dev.078220 (2012).
45 Du, H. & Taylor, H. S. The Role of Hox Genes in Female Reproductive Tract Development, Adult Function, and Fertility. *Cold Spring Harb Perspect Med* **6**, a023002, doi:10.1101/cshperspect.a023002 (2015).
46 Cakmak, H. & Taylor, H. S. Molecular mechanisms of treatment resistance in endometriosis: the role of progesterone-hox gene interactions. *Semin Reprod Med* **28**, 69-74, doi:10.1055/s-0029-1242996 (2010).
47 Taylor, H. S., Bagot, C., Kardana, A., Olive, D. & Arici, A. HOX gene expression is altered in the endometrium of women with endometriosis. *Hum Reprod* **14**, 1328-1331, doi:10.1093/humrep/14.5.1328 (1999).

745 48 He, B., Ni, Z. L., Kong, S. B., Lu, J. H. & Wang, H. B. Homeobox genes for embryo implantation:
746 From mouse to human. *Animal Model Exp Med* **1**, 14-22, doi:10.1002/ame2.12002 (2018).
747 49 Illingworth, I. M. *et al.* Desmosomes are reduced in the mouse uterine luminal epithelium during
748 the preimplantation period of pregnancy: a mechanism for facilitation of implantation. *Biol Reprod*
749 **63**, 1764-1773, doi:10.1095/biolreprod63.6.1764 (2000).
750 50 Paria, B. C., Zhao, X., Das, S. K., Dey, S. K. & Yoshinaga, K. Zonula occludens-1 and E-cadherin
751 are coordinately expressed in the mouse uterus with the initiation of implantation and
752 decidualization. *Dev Biol* **208**, 488-501, doi:10.1006/dbio.1999.9206 (1999).
753 51 Potter, S. W., Gaza, G. & Morris, J. E. Estradiol induces E-cadherin degradation in mouse uterine
754 epithelium during the estrous cycle and early pregnancy. *J Cell Physiol* **169**, 1-14,
755 doi:10.1002/(SICI)1097-4652(199610)169:1<1::AID-JCP1>3.0.CO;2-S (1996).
756 52 Grund, S. & Grummer, R. Direct Cell(-)Cell Interactions in the Endometrium and in Endometrial
757 Pathophysiology. *Int J Mol Sci* **19**, doi:10.3390/ijms19082227 (2018).
758 53 Schatz, F., Guzeloglu-Kayisli, O., Arlier, S., Kayisli, U. A. & Lockwood, C. J. The role of decidual
759 cells in uterine hemostasis, menstruation, inflammation, adverse pregnancy outcomes and
760 abnormal uterine bleeding. *Hum Reprod Update* **22**, 497-515, doi:10.1093/humupd/dmw004
761 (2016).
762 54 Evans, J. *et al.* Fertile ground: human endometrial programming and lessons in health and
763 disease. *Nat Rev Endocrinol* **12**, 654-667, doi:10.1038/nrendo.2016.116 (2016).
764 55 Stehlin-Gaon, C. *et al.* All-trans retinoic acid is a ligand for the orphan nuclear receptor ROR beta.
765 *Nat Struct Biol* **10**, 820-825, doi:10.1038/nsb979 (2003).
766 56 Spitzer, T. L. *et al.* Perivascular human endometrial mesenchymal stem cells express pathways
767 relevant to self-renewal, lineage specification, and functional phenotype. *Biol Reprod* **86**, 58,
768 doi:10.1095/biolreprod.111.095885 (2012).
769 57 Yin, Y., Haller, M. E., Chadchan, S. B., Kommagani, R. & Ma, L. Signaling through retinoic acid
770 receptors is essential for mammalian uterine receptivity and decidualization. *JCI Insight* **6**,
771 doi:10.1172/jci.insight.150254 (2021).
772 58 Chang, C. Agonists and Antagonists of TGF-beta Family Ligands. *Cold Spring Harb Perspect Biol*
773 **8**, doi:10.1101/cshperspect.a021923 (2016).
774 59 Fullerton, P. T., Jr., Monsivais, D., Kommagani, R. & Matzuk, M. M. Follistatin is critical for mouse
775 uterine receptivity and decidualization. *Proc Natl Acad Sci U S A* **114**, E4772-E4781,
776 doi:10.1073/pnas.1620903114 (2017).
777 60 Li, Q. *et al.* The antiproliferative action of progesterone in uterine epithelium is mediated by
778 Hand2. *Science* **331**, 912-916, doi:10.1126/science.1197454 (2011).
779 61 Filant, J., DeMayo, F. J., Pru, J. K., Lydon, J. P. & Spencer, T. E. Fibroblast growth factor
780 receptor two (FGFR2) regulates uterine epithelial integrity and fertility in mice. *Biol Reprod* **90**, 7,
781 doi:10.1095/biolreprod.113.114496 (2014).
782 62 Lim, W., Bae, H., Bazer, F. W. & Song, G. Stimulatory effects of fibroblast growth factor 2 on
783 proliferation and migration of uterine luminal epithelial cells during early pregnancy. *Biol Reprod*
784 **96**, 185-198, doi:10.1095/biolreprod.116.142331 (2017).
785 63 Russo, L. A. *et al.* Regulated expression of matrix metalloproteinases, inflammatory mediators,
786 and endometrial matrix remodeling by 17beta-estradiol in the immature rat uterus. *Reprod Biol*
787 *Endocrinol* **7**, 124, doi:10.1186/1477-7827-7-124 (2009).
788 64 Tenvergert, E., Gillespie, M. W., Kingma, J. & Klasen, H. Abortion attitudes, 1984-1987-1988:
789 effects of item order and dimensionality. *Percept Mot Skills* **74**, 627-642,
790 doi:10.2466/pms.1992.74.2.627 (1992).
791 65 Hayashi, K. *et al.* Wnt genes in the mouse uterus: potential regulation of implantation. *Biol*
792 *Reprod* **80**, 989-1000, doi:10.1095/biolreprod.108.075416 (2009).
793 66 Garcia-Alonso, L. *et al.* Mapping the temporal and spatial dynamics of the human endometrium in
794 vivo and in vitro. *Nat Genet* **53**, 1698-1711, doi:10.1038/s41588-021-00972-2 (2021).
795 67 PrabhuDas, M. *et al.* Immune mechanisms at the maternal-fetal interface: perspectives and
796 challenges. *Nat Immunol* **16**, 328-334, doi:10.1038/ni.3131 (2015).

797 68 Guimaraes-Young, A., Neff, T., Dupuy, A. J. & Goodheart, M. J. Conditional deletion of Sox17
798 reveals complex effects on uterine adenogenesis and function. *Dev Biol* **414**, 219-227,
799 doi:10.1016/j.ydbio.2016.04.010 (2016).
800 69 Hirate, Y. *et al.* Mouse Sox17 haploinsufficiency leads to female subfertility due to impaired
801 implantation. *Sci Rep* **6**, 24171, doi:10.1038/srep24171 (2016).
802 70 Wang, X. *et al.* SOX17 regulates uterine epithelial-stromal cross-talk acting via a distal enhancer
803 upstream of Ihh. *Nat Commun* **9**, 4421, doi:10.1038/s41467-018-06652-w (2018).
804 71 Hollnagel, A., Oehlmann, V., Heymer, J., Ruther, U. & Nordheim, A. Id genes are direct targets of
805 bone morphogenetic protein induction in embryonic stem cells. *J Biol Chem* **274**, 19838-19845,
806 doi:10.1074/jbc.274.28.19838 (1999).
807 72 Miyazono, K. & Miyazawa, K. Id: a target of BMP signaling. *Sci STKE* **2002**, pe40,
808 doi:10.1126/stke.2002.151.pe40 (2002).
809 73 Holloran, S. M. *et al.* Reciprocal fine-tuning of progesterone and prolactin-regulated gene
810 expression in breast cancer cells. *Mol Cell Endocrinol* **511**, 110859,
811 doi:10.1016/j.mce.2020.110859 (2020).
812 74 Dinh, D. T. *et al.* Progesterone receptor mediates ovulatory transcription through RUNX
813 transcription factor interactions and chromatin remodelling. *Nucleic Acids Res*,
814 doi:10.1093/nar/gkad271 (2023).
815 75 Vasquez, Y. M. *et al.* FOXO1 regulates uterine epithelial integrity and progesterone receptor
816 expression critical for embryo implantation. *PLoS Genet* **14**, e1007787,
817 doi:10.1371/journal.pgen.1007787 (2018).
818 76 Shi, J. W. *et al.* An IGF1-expressing endometrial stromal cell population is associated with human
819 decidualization. *BMC Biol* **20**, 276, doi:10.1186/s12915-022-01483-0 (2022).
820 77 Suzuki, A. *et al.* Nanog binds to Smad1 and blocks bone morphogenetic protein-induced
821 differentiation of embryonic stem cells. *Proc Natl Acad Sci U S A* **103**, 10294-10299,
822 doi:10.1073/pnas.0506945103 (2006).
823 78 Shi, X., Bai, S., Li, L. & Cao, X. Hoxa-9 represses transforming growth factor-beta-induced
824 osteopontin gene transcription. *J Biol Chem* **276**, 850-855, doi:10.1074/jbc.M005955200 (2001).
825 79 Shi, X., Yang, X., Chen, D., Chang, Z. & Cao, X. Smad1 interacts with homeobox DNA-binding
826 proteins in bone morphogenetic protein signaling. *J Biol Chem* **274**, 13711-13717,
827 doi:10.1074/jbc.274.19.13711 (1999).
828 80 Feng, X. H. & Derynck, R. Specificity and versatility in tgf-beta signaling through Smads. *Annu*
829 *Rev Cell Dev Biol* **21**, 659-693, doi:10.1146/annurev.cellbio.21.022404.142018 (2005).
830 81 Massague, J., Seoane, J. & Wotton, D. Smad transcription factors. *Genes Dev* **19**, 2783-2810,
831 doi:10.1101/gad.1350705 (2005).
832 82 Derynck, R. & Budi, E. H. Specificity, versatility, and control of TGF-beta family signaling. *Sci*
833 *Signal* **12**, doi:10.1126/scisignal.aav5183 (2019).
834 83 Lee, D. K. *et al.* Suppression of ERalpha activity by COUP-TFII is essential for successful
835 implantation and decidualization. *Mol Endocrinol* **24**, 930-940, doi:10.1210/me.2009-0531 (2010).
836 84 Vasquez, Y. M. *et al.* FOXO1 is required for binding of PR on IRF4, novel transcriptional regulator
837 of endometrial stromal decidualization. *Mol Endocrinol* **29**, 421-433, doi:10.1210/me.2014-1292
838 (2015).
839 85 Wu, M., Chen, G. & Li, Y. P. TGF-beta and BMP signaling in osteoblast, skeletal development,
840 and bone formation, homeostasis and disease. *Bone Res* **4**, 16009, doi:10.1038/boneres.2016.9
841 (2016).
842 86 van Weerd, J. H. & Christoffels, V. M. The formation and function of the cardiac conduction
843 system. *Development* **143**, 197-210, doi:10.1242/dev.124883 (2016).
844 87 Whitman, M. Smads and early developmental signaling by the TGFbeta superfamily. *Genes Dev*
845 **12**, 2445-2462, doi:10.1101/gad.12.16.2445 (1998).
846 88 Middlebrook, B. S., Eldin, K., Li, X., Shivasankaran, S. & Pangas, S. A. Smad1-Smad5 ovarian
847 conditional knockout mice develop a disease profile similar to the juvenile form of human
848 granulosa cell tumors. *Endocrinology* **150**, 5208-5217, doi:10.1210/en.2009-0644 (2009).

89 Pangas, S. A. *et al.* Conditional deletion of Smad1 and Smad5 in somatic cells of male and female gonads leads to metastatic tumor development in mice. *Mol Cell Biol* **28**, 248-257, doi:10.1128/MCB.01404-07 (2008).
90 Rodriguez, A. *et al.* SMAD Signaling Is Required for Structural Integrity of the Female Reproductive Tract and Uterine Function During Early Pregnancy in Mice. *Biol Reprod* **95**, 44, doi:10.1095/biolreprod.116.139477 (2016).
91 Retting, K. N., Song, B., Yoon, B. S. & Lyons, K. M. BMP canonical Smad signaling through Smad1 and Smad5 is required for endochondral bone formation. *Development* **136**, 1093-1104, doi:10.1242/dev.029926 (2009).
92 McReynolds, L. J., Gupta, S., Figueroa, M. E., Mullins, M. C. & Evans, T. Smad1 and Smad5 differentially regulate embryonic hematopoiesis. *Blood* **110**, 3881-3890, doi:10.1182/blood-2007-04-085753 (2007).
93 Consortium, E. P. An integrated encyclopedia of DNA elements in the human genome. *Nature* **489**, 57-74, doi:10.1038/nature11247 (2012).
94 Chen, J. *et al.* Single-molecule dynamics of enhanceosome assembly in embryonic stem cells. *Cell* **156**, 1274-1285, doi:10.1016/j.cell.2014.01.062 (2014).
95 Swinstead, E. E. *et al.* Steroid Receptors Reprogram FoxA1 Occupancy through Dynamic Chromatin Transitions. *Cell* **165**, 593-605, doi:10.1016/j.cell.2016.02.067 (2016).
96 Chen, C. H. *et al.* Determinants of transcription factor regulatory range. *Nat Commun* **11**, 2472, doi:10.1038/s41467-020-16106-x (2020).
97 Arvey, A., Agius, P., Noble, W. S. & Leslie, C. Sequence and chromatin determinants of cell-type-specific transcription factor binding. *Genome Res* **22**, 1723-1734, doi:10.1101/gr.127712.111 (2012).
98 Tang, S., Cope, D. I., Vasquez, Y. M. & Monsivais, D. BMP/SMAD1/5 Signaling in the Endometrial Epithelium Is Essential for Receptivity and Early Pregnancy. *Endocrinology* **163**, doi:10.1210/endocr/bqac043 (2022).
99 Newman, A. M. *et al.* Determining cell type abundance and expression from bulk tissues with digital cytometry. *Nat Biotechnol* **37**, 773-782, doi:10.1038/s41587-019-0114-2 (2019).
100 Fuentealba, L. C. *et al.* Integrating patterning signals: Wnt/GSK3 regulates the duration of the BMP/Smad1 signal. *Cell* **131**, 980-993, doi:10.1016/j.cell.2007.09.027 (2007).
101 Labbe, E., Letamendia, A. & Attisano, L. Association of Smads with lymphoid enhancer binding factor 1/T cell-specific factor mediates cooperative signaling by the transforming growth factor-beta and wnt pathways. *Proc Natl Acad Sci U S A* **97**, 8358-8363, doi:10.1073/pnas.150152697 (2000).
102 Zavadil, J., Cermak, L., Soto-Nieves, N. & Bottinger, E. P. Integration of TGF-beta/Smad and Jagged1/Notch signalling in epithelial-to-mesenchymal transition. *EMBO J* **23**, 1155-1165, doi:10.1038/sj.emboj.7600069 (2004).
103 Qiu, T., Grizzle, W. E., Oelschlager, D. K., Shen, X. & Cao, X. Control of prostate cell growth: BMP antagonizes androgen mitogenic activity with incorporation of MAPK signals in Smad1. *EMBO J* **26**, 346-357, doi:10.1038/sj.emboj.7601499 (2007).
104 Luo, K. *et al.* The Ski oncoprotein interacts with the Smad proteins to repress TGFbeta signaling. *Genes Dev* **13**, 2196-2206, doi:10.1101/gad.13.17.2196 (1999).
105 Pouponnot, C., Jayaraman, L. & Massague, J. Physical and functional interaction of SMADs and p300/CBP. *J Biol Chem* **273**, 22865-22868, doi:10.1074/jbc.273.36.22865 (1998).
106 Brosens, J. J. & Gellersen, B. Death or survival--progesterone-dependent cell fate decisions in the human endometrial stroma. *J Mol Endocrinol* **36**, 389-398, doi:10.1677/jme.1.02060 (2006).
107 Yilmaz, B. D. & Bulun, S. E. Endometriosis and nuclear receptors. *Hum Reprod Update* **25**, 473-485, doi:10.1093/humupd/dmz005 (2019).
108 Janzen, D. M. *et al.* Progesterone receptor signaling in the microenvironment of endometrial cancer influences its response to hormonal therapy. *Cancer Res* **73**, 4697-4710, doi:10.1158/0008-5472.CAN-13-0930 (2013).
109 MacLean, J. A., 2nd & Hayashi, K. Progesterone Actions and Resistance in Gynecological Disorders. *Cells* **11**, doi:10.3390/cells11040647 (2022).

902

903

904

905 **TABLE AND FIGURES LEGENDS**

Figure 1

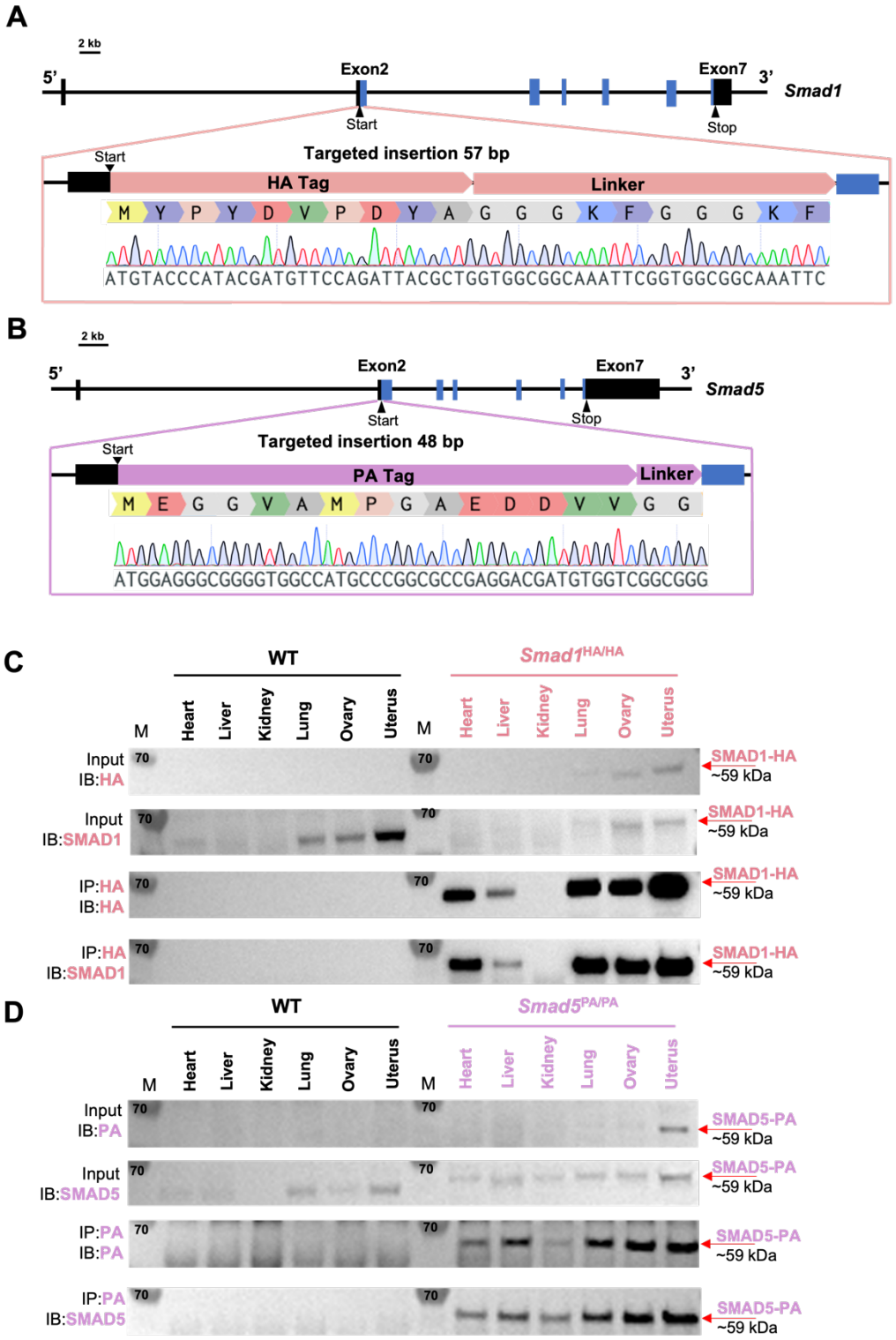

906 **Figure 1: Mouse models with global HA tagged SMAD1 and PA tagged SMAD5 proteins. A-B**)

907 Schematic approaches for generating Smad1HA/HA and Smad5PA/PA knock-in mouse lines. Sanger

908 sequencing of the genotyping results are included as validation of knock-in sequence. Black and blue
909 boxes indicate untranslated and coding regions, respectively. **C-D)** Immunoblot (IB) analysis of the
910 immunoprecipitation (IP) of HA tagged SMAD1 and PA tagged SMAD5 proteins from different tissues of
911 the tagged mouse lines. Wild type (WT) mice were used as negative controls. Antibodies used for IB and
912 IP are as labeled. Targeted bands of SMAD1 and SMAD5 are indicated by red arrows.

Figure 2

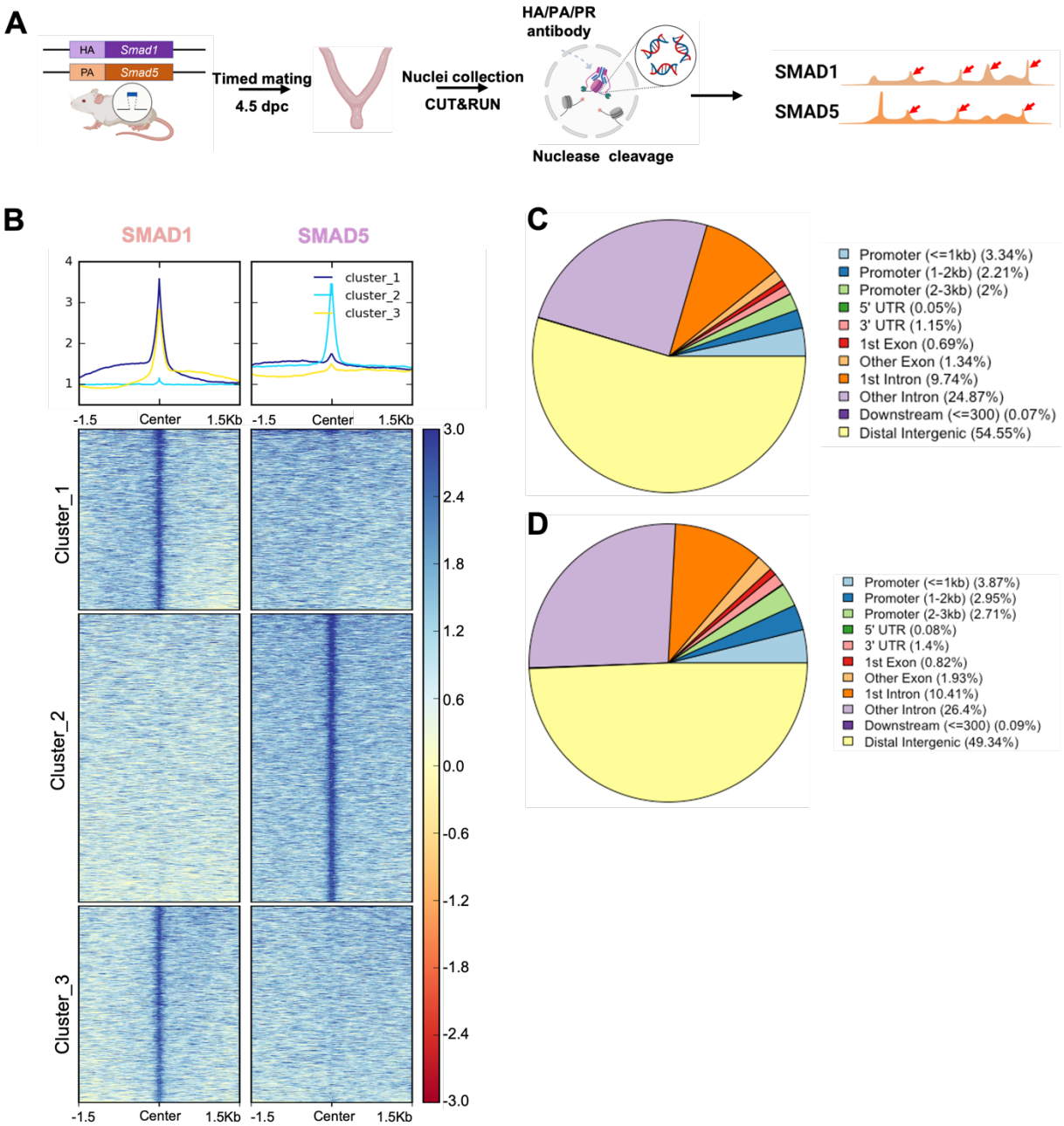

Figure 2: Genomic profiling of SMAD1 and SMAD5 binding sites during decidualization *in vivo*. A) Diagram outlining experimental approaches for tissue collection, processing, and CUT&RUN. **B**) Heatmaps and summary plots showing the enrichment of SMAD1 and SMAD5 binding peaks from one exemplary replicate. Clustering was conducted using k-means algorithm. The colors in the summary plots correspond to clusters labeled in the heatmap below. **C-D**) Feature distribution of the annotated peaks for the SMAD1 (C) binding sites and SMAD5 (D) binding sites.

Figure 3

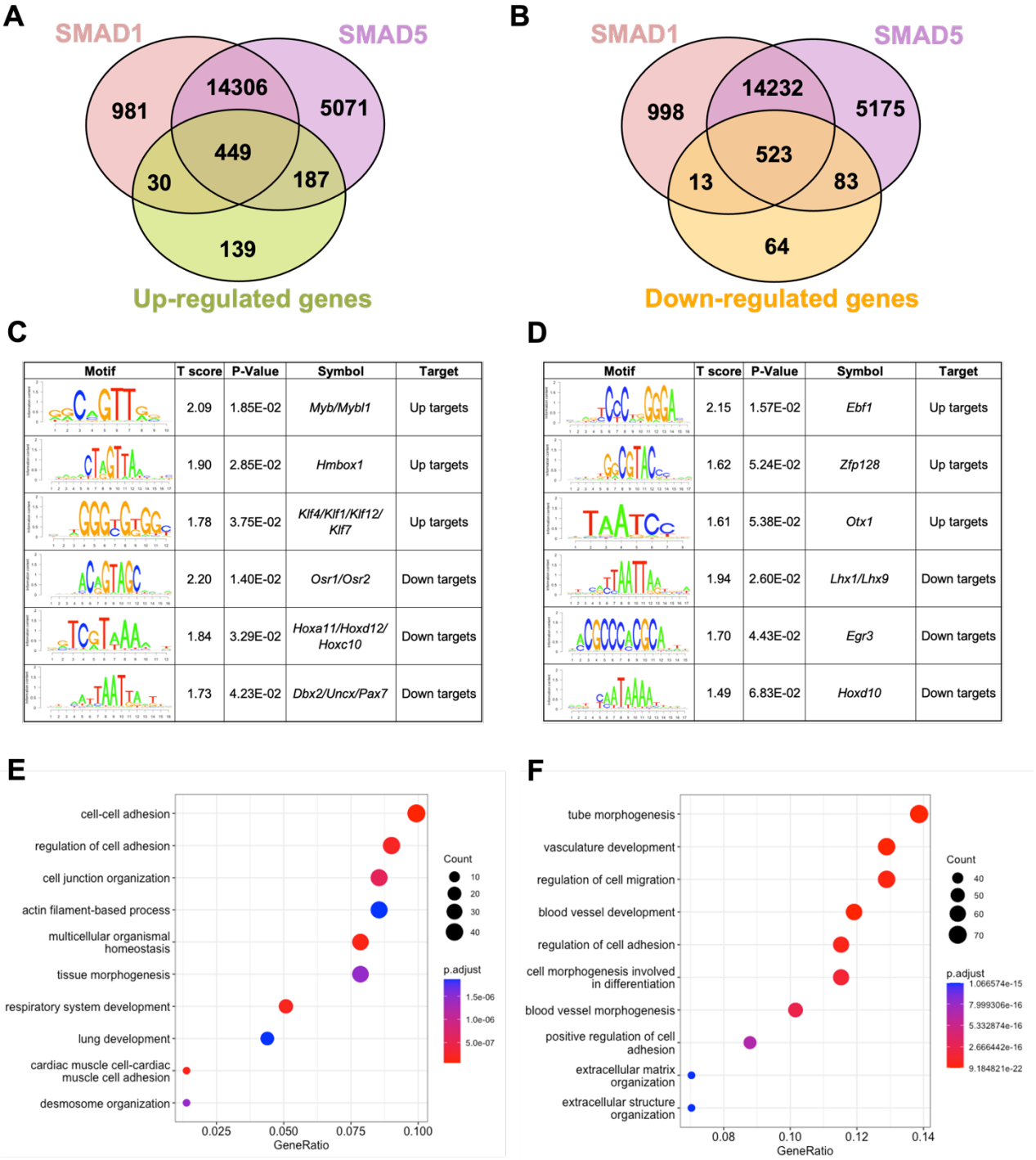

Motif	T score	P-Value	Symbol	Target
	2.09	1.85E-02	*Myb/Mybl1*	Up targets
	1.90	2.85E-02	*Hmbox1*	Up targets
	1.78	3.75E-02	*Klf4/Klf1/Klf12/ Klf7*	Up targets
	2.20	1.40E-02	*Osr1/Osr2*	Down targets
	1.84	3.29E-02	*Hoxa11/Hoxd12/ Hoxc10*	Down targets
	1.73	4.23E-02	*Dbx2/Uncx/Pax7*	Down targets

Motif	T score	P-Value	Symbol	Target
	2.15	1.57E-02	*Ebf1*	Up targets
	1.62	5.24E-02	*Zfp128*	Up targets
	1.61	5.38E-02	*Otx1*	Up targets
	1.94	2.60E-02	*Lhx1/Lhx9*	Down targets
	1.70	4.43E-02	*Egr3*	Down targets
	1.49	6.83E-02	*Hoxd10*	Down targets

Figure 3: SMAD1 and SMAD5 show unique direct target genes during early pregnancy. A-B) Venn diagrams showing the shared and unique direct up-target genes (A) and down-target genes (B) of SMAD1, SMAD5 Numbers indicate genes numbers. **C-D**) Motif enrichment analysis from the up-targets and down-targets for SMAD1 (C) and SMAD5 (D). **E-F**) Dot plot showing Gene Ontology enrichment

923 analysis of shared direct target genes of SMAD1/5 from the up-targets (E) and the down-targets (F),
924 respectively. Dot size represents the gene ratio in the enriched categories compared to background
925 genes, dot colors reflect P-value.

926

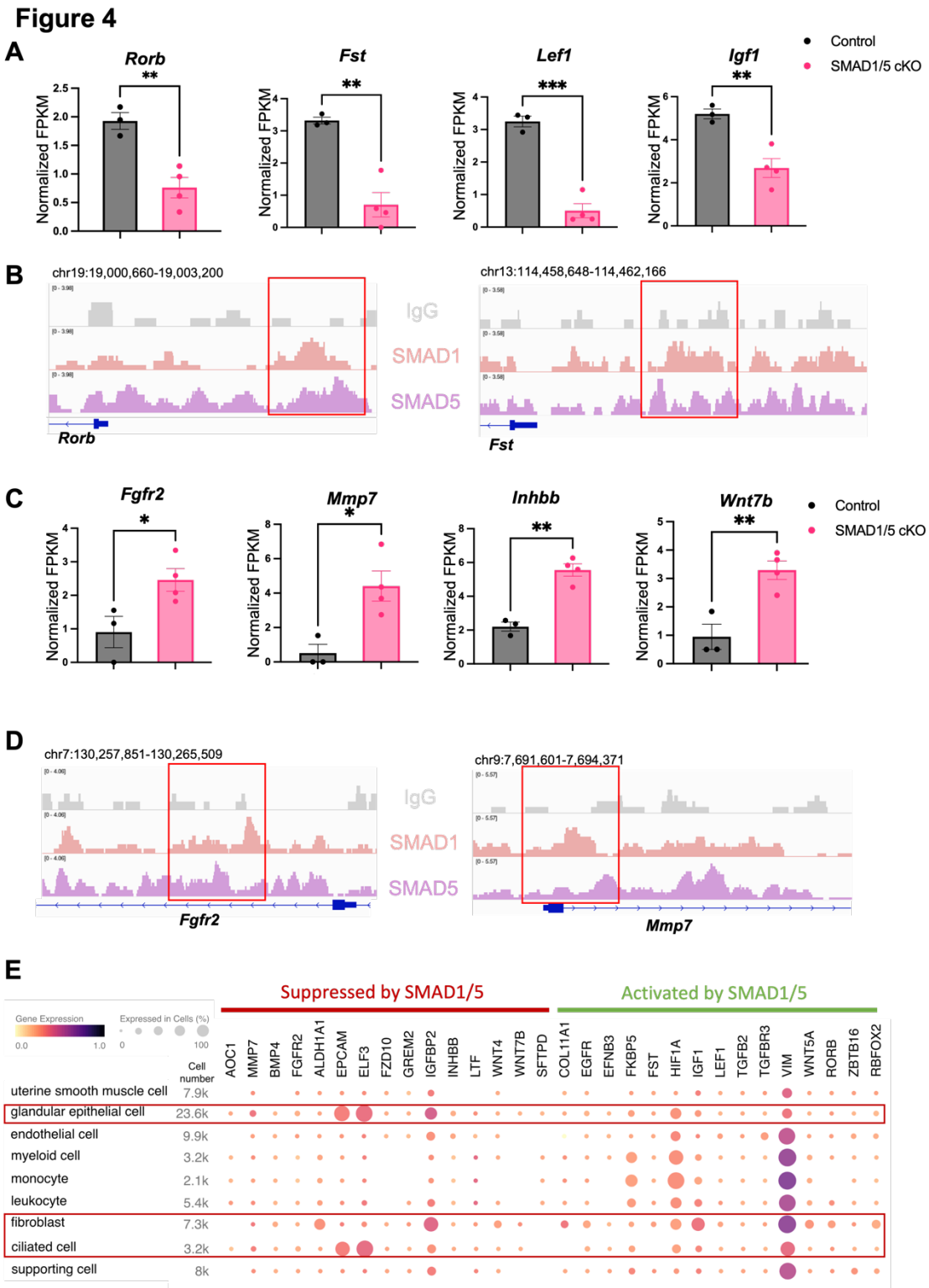

Figure 4: Direct target genes of SMAD1/5 mediate uterine homeostasis. **A**) Bar graph of normalized Fragments Per Kilobase of transcript per Million mapped reads (FPKM) of downregulated transcripts in the Control and SMAD1/5 cKO groups as indicated by the label. Histograms represent average +/- SEM of experiments uteri from Control mice (N=3) and SMAD1/5 cKO mice (N=4). Analyzed by a unpaired t-

931 test. **B**) Integrative Genomics Viewer (IGV) track view of SMAD1, SMAD5 binding activities. Gene loci
932 are as indicated in the figure, genomic coordinates are annotated in mm10. **C**) Bar graph of FPKM of up
933 regulated transcripts in the Control and SMAD1/5 cKO groups as indicated by the label. **D**) IGV track
934 view of SMAD1, SMAD5 binding activities. Gene loci are as indicated in the figure, genomic coordinates
935 are annotated in mm10. **E**) Dot plot showing the gene expression pattern of the key SMAD1/5 direct
936 target genes in different cell types from published human endometrium single-cell RNA-seq dataset.

Figure 5

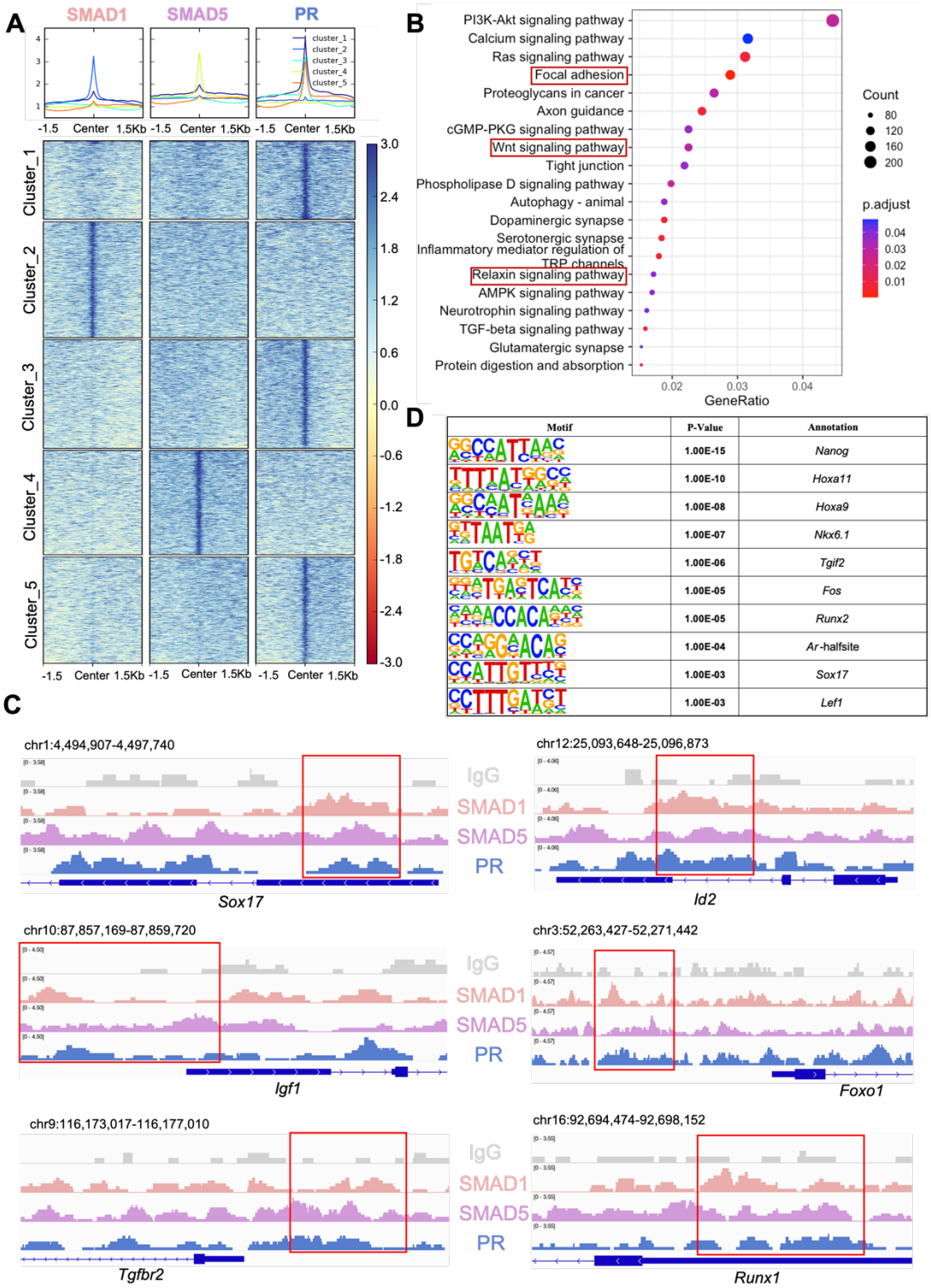

Figure 5: SMAD1 and SMAD5 co-regulate PR target genes. A) Heatmaps and summary plots showing the enrichment comparison between SMAD1, SMAD5 and PR binding peaks from one exemplary replicate. Clustering was conducted using k-means algorithm. The colors in the summary

941 plots correspond to clusters labeled in the heatmap below. **B**) Dot plot showing KEGG pathway
942 enrichment analysis for shared genes bound by SMAD1, SMAD5, and PR. **C**) IGV track view of SMAD1,
943 SMAD5 and PR binding activities. Gene loci are as indicated in the figure, genomic coordinates are
944 annotated in mm10. **D**) Table of motif analysis results for shared peaks between SMAD1, SMAD5 and
945 PR, with P-value and motif annotation specified for each motif.

946

Figure 6

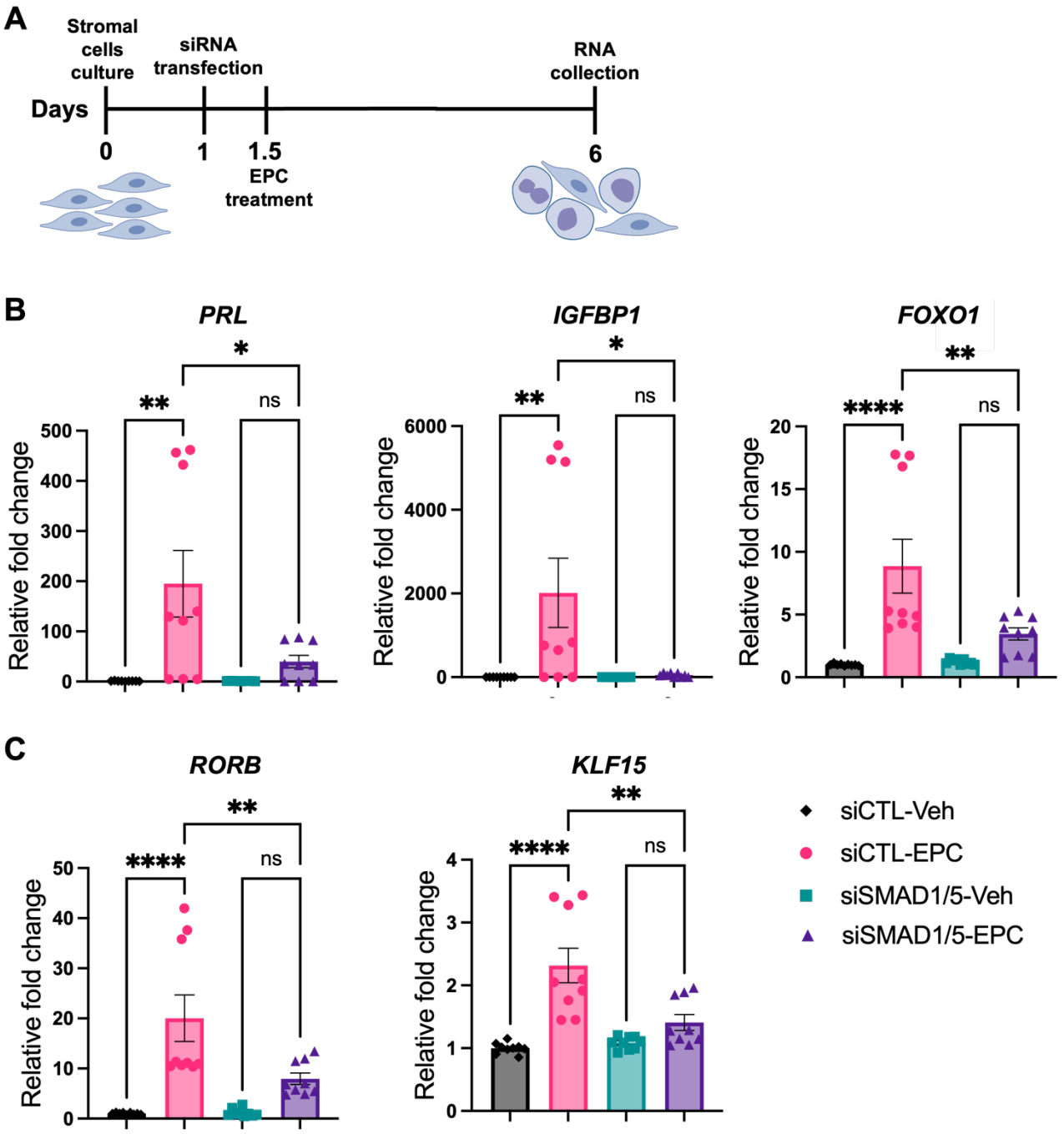

947

948 **Figure 6: SMAD1 and SMAD5 are required for PR responses during decidualization of human**

949 **endometrial stromal cells. A**) Schematic approach and timeline outlining in vitro decidualization for

950 endometrial stromal cells (EnSCs). **B-C**) RT-qPCR results showing mRNA levels of *PRL*, *IGFBP1*,

951 *FOXO1*, *RORB* and *KLF15* after SMAD1/5 perturbation using siRNAs. Data are normalized to siCTL-Veh

952 for visualization. Bar graphs represent average +/- SEM of experiments on cells from three different

953 individuals with technical triplicates. Analyzed by a One-Way ANOVA test with post hoc Tukey test.

954

Supplement Figure 1:

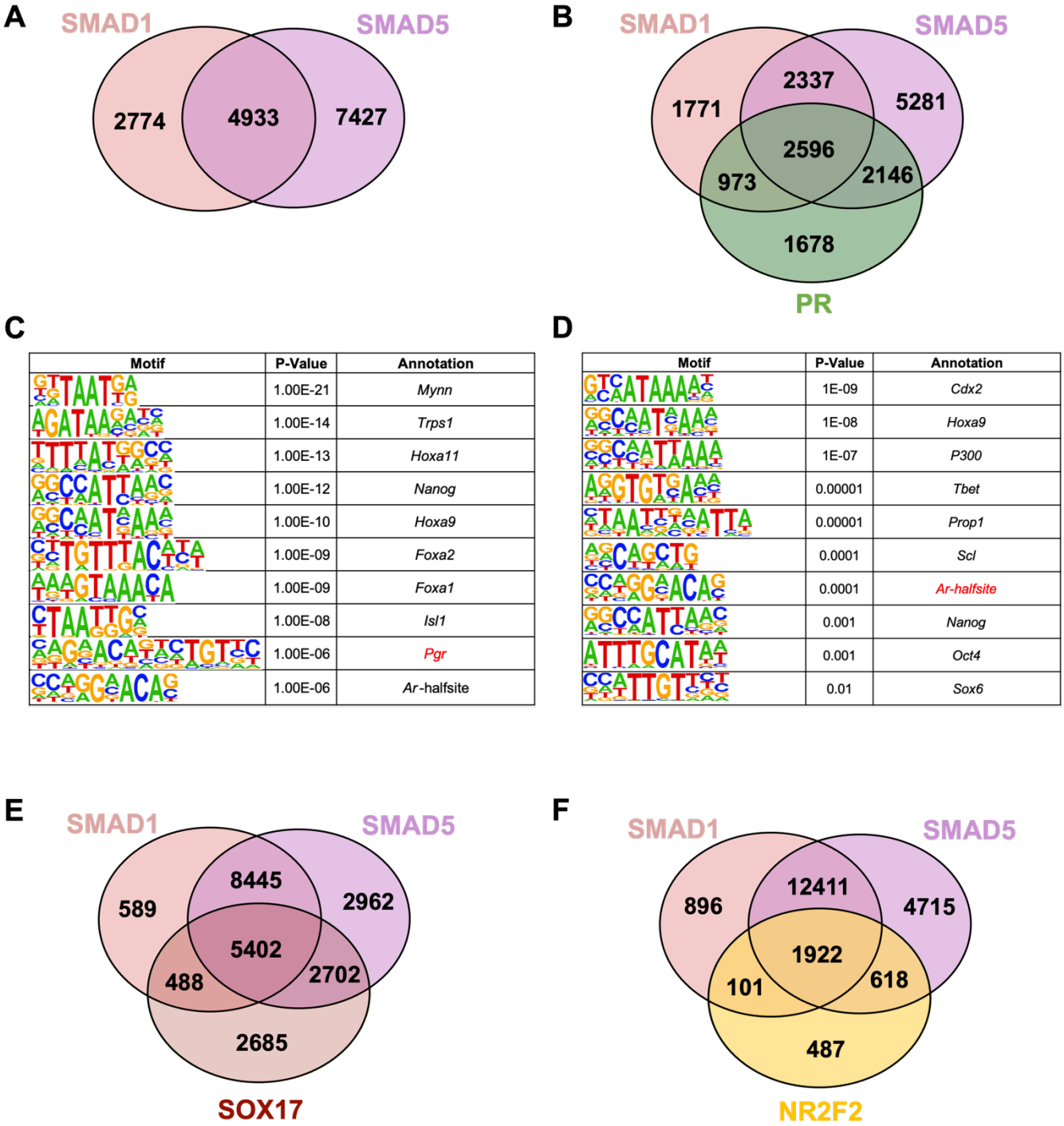

Motif	P-Value	Annotation
	1.00E-21	*Mynn*
	1.00E-14	*Trps1*
	1.00E-13	*Hoxa11*
	1.00E-12	*Nanog*
	1.00E-10	*Hoxa9*
	1.00E-09	*Foxa2*
	1.00E-09	*Foxa1*
	1.00E-08	*Isl1*
	1.00E-06	*Pgr*
	1.00E-06	*Ar*-halfsite

Motif	P-Value	Annotation
	1E-09	*Cdx2*
	1E-08	*Hoxa9*
	1E-07	*P300*
	0.00001	*Tbet*
	0.00001	*Prop1*
	0.0001	*Scl*
	0.0001	*Ar-halfsite*
	0.001	*Nanog*
	0.001	*Oct4*
	0.01	*Sox6*

Supplement Figure 1: Gene numbers with SMAD1/5 promoter binding activities and motif analysis of SMAD1/5 peaks. A) Venn diagrams showing the shared and unique genes bound by SMAD1 or SMAD5 in the +/- 3kb region of the promoter regions. **B**) Venn diagrams showing the shared and unique genes bound by SMAD1, SMAD5 or PR in the +/- 3kb of the promoter regions. **C-D**) Table of

960 motif analysis results for unique peaks for SMAD1(C) and SMAD5 (D), with P-value and motif annotation
961 specified for each motif. **E)** Venn diagrams showing the shared and unique genes bound by SMAD1,
962 SMAD5 or SOX17 in the +/- 25kb regions near transcription start site. **F)** Venn diagrams showing the
963 shared and unique genes bound by SMAD1, SMAD5 or NR2F2 in the +/- 25kb regions near transcription
964 start site.

Supplement Figure 2:

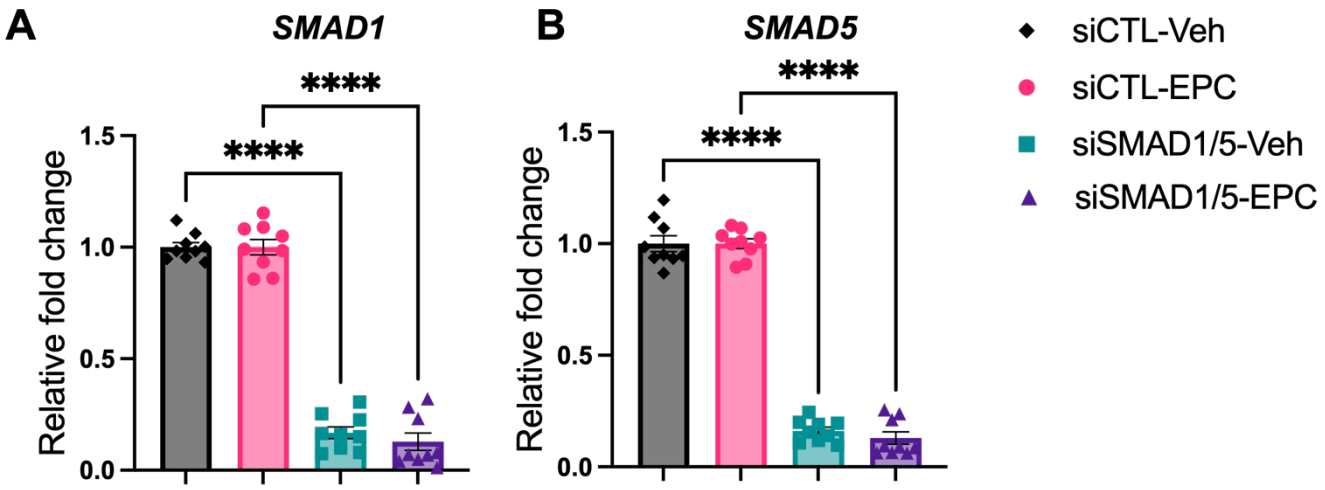

Supplement Figure 2: Knockdown effect validation of SMAD1/5 perturbation. A-B) RT-qPCR results showing mRNA levels of SMAD1(A) and SMAD5 (B) after siRNA treatments in the both Veh and EPC conditions. Data are normalized to siCTL for visualization. Bar graphs represent average +/- SEM of experiments on cells from three different individuals with technical triplicates. Analyzed by a One-Way ANOVA test with post hoc Tukey test.

Supplement Figure 3:

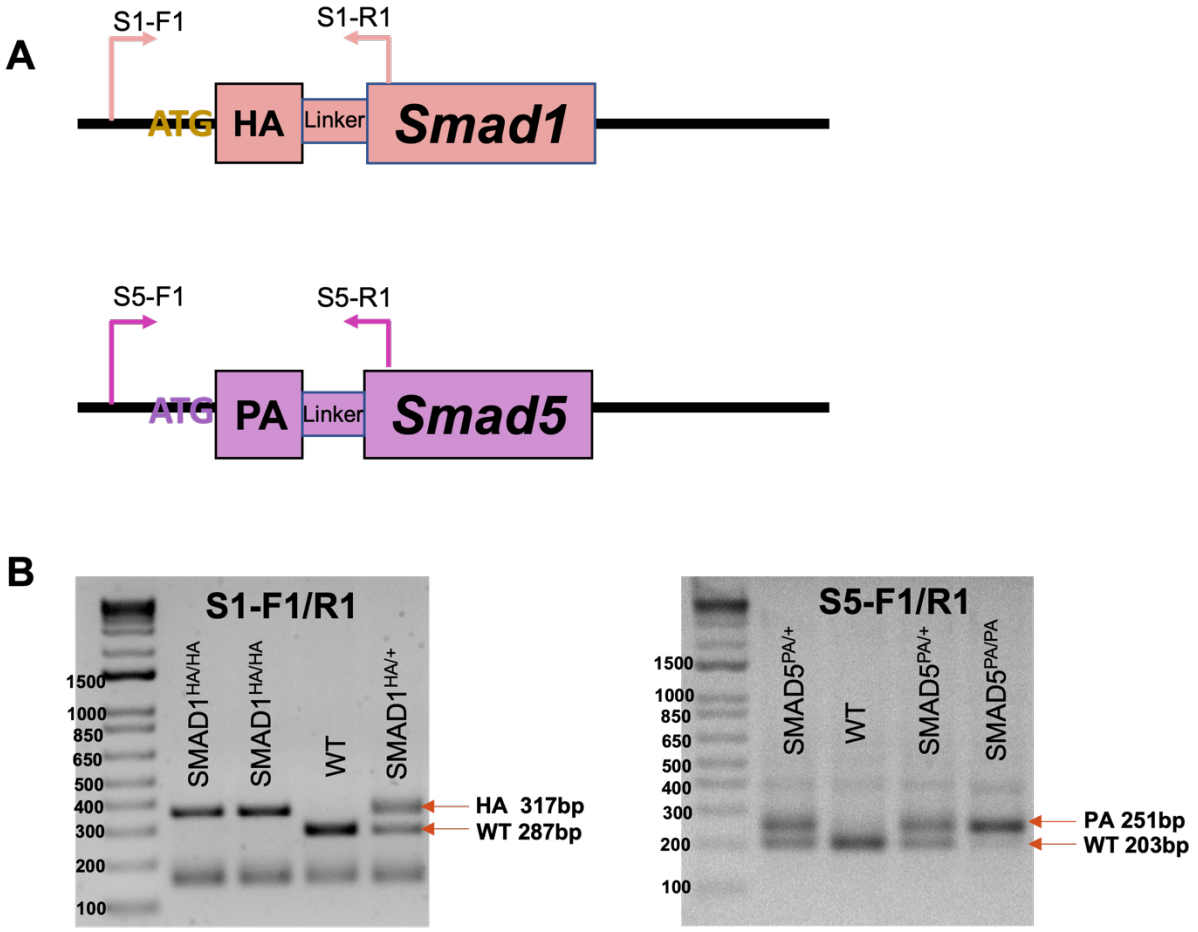

Supplement Figure 3: Genotype of the knock-in mouse lines. **A**) Schematic design of the genotype primers for Smad1HA/HA and Smad5PA/PA mouse lines. **B**) Exemplary gel electrophoresis of PCR products derived from homozygous knock-in mice, heterozygous mice, and WT mice using genotyping primers.

Uncropped Western Blots for Figure 1

A

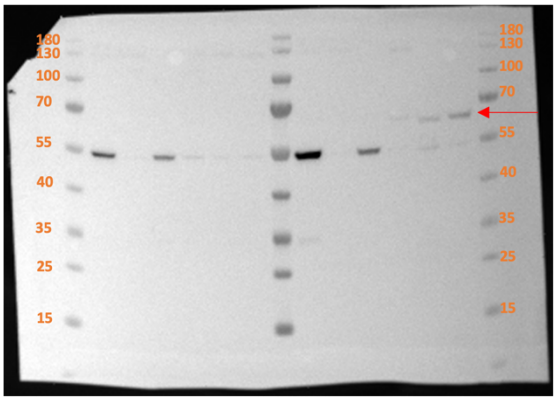

B

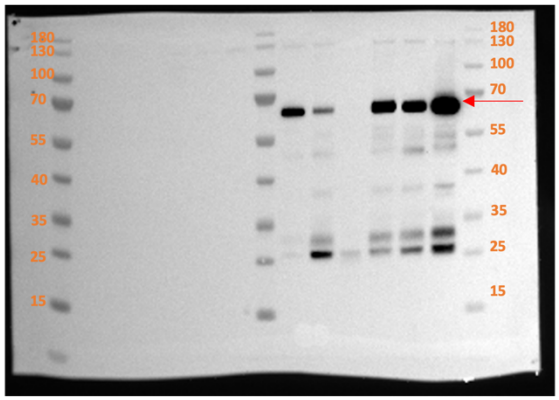

C

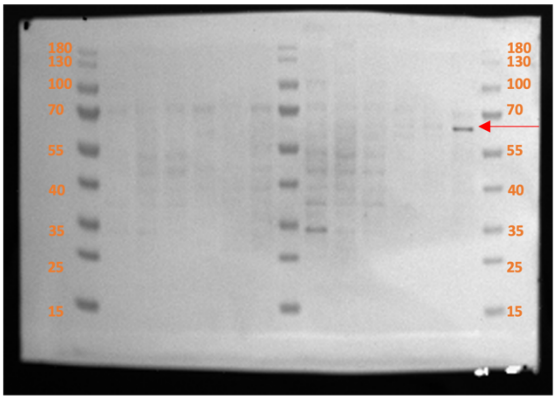

D

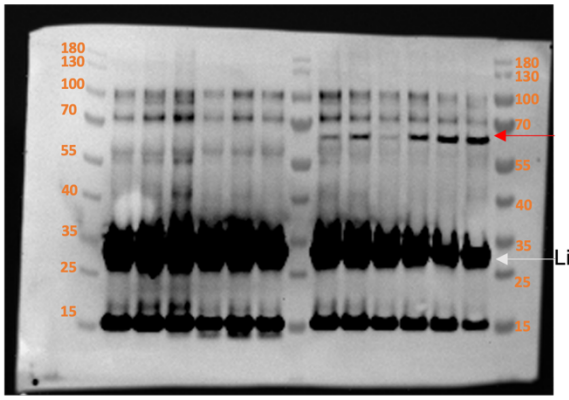

E

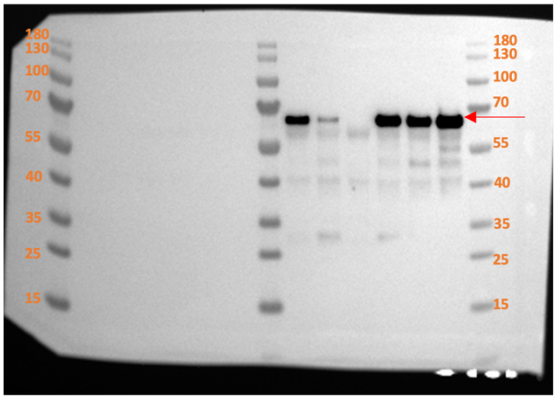
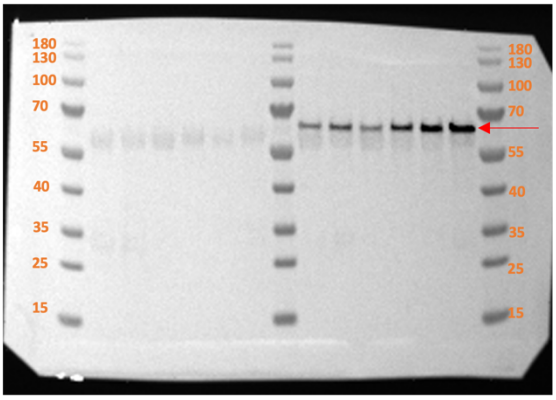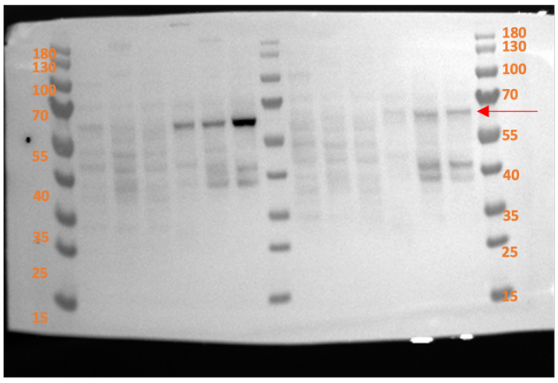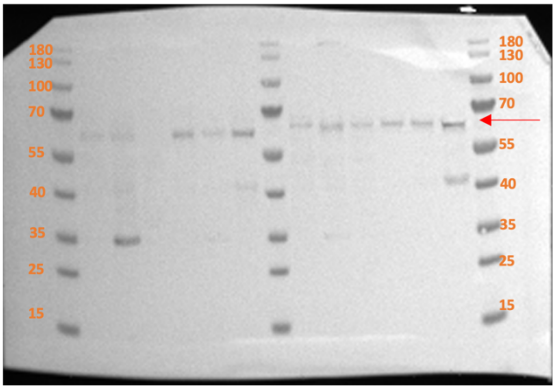
F